OUKA
Osaka University Knowledge Archive

Title	Analysis of Polyunsaturated Fatty Acids by Electrospray Ionization Mass Spectrometry
Author(s)	Zhu, Huibin
Citation	大阪大学, 2023, 博士論文
Version Type	VoR
URL	https://doi.org/10.18910/93021
rights	
Note	

Osaka University Knowledge Archive : OUKA

https://ir.library.osaka-u.ac.jp/

Osaka University

Analysis of Polyunsaturated Fatty Acids by Electrospray Ionization Mass Spectrometry

Huibin Zhu

Department of Chemistry
Graduate School of Science
Osaka University

2023

Index

Chapters 2 and 3 of this dissertation describe the contents published in the paper (Zhu H, et al. J. Lipid Res., https://www.jlr.org/article/S0022-2275(23)00057-3/fulltext) with some modifications.

Abbreviations

ACN	Acetonitrile
MeOH	Methanol
TFA	Trifluoroacetic acid
DIEA	N, N-diisopropylethylamine
TEA	Triethylamine
DMF	Dimethylformamide
HBTU	1-[Bis (dimethylamino) methylene]-1H-benzotriazolium 3-Oxide Hexafluorophosphate
BHT	2, 6-di-tert-butyl-4-methylphenol
DMED	N, N -Dimethylethylenediamine
TEA	Trimethylamine
CMPI	2-chloro-1-methylpyridinium iodide
FA	Formic acid
PUFA	Polyunsaturated fatty acid
ARA	Arachidonic acid
DHA	Docosahexaenoic acid
EPA	Eicosapentaenoic acid
HETE	Hydroxyeicosatetraenoic acid
HDoHE	Hydroxy docosahexaenoic acid
Rv	Resolvin
Lx	Lipoxin
ESI	Electrospray ionization
MS	Mass spectrometry
LC	Liquid Chromatography
HPLC/UPLC	High/Ultra-performance liquid chromatography
CID	Collision-Induced Dissociation
RT	Retention time

General Introduction

1. An Overview of Polyunsaturated Fatty Acids

1.1 Classification and Key Metabolic Products of Polyunsaturated Fatty Acids

Fatty acids are a class of compounds consisting of hydrocarbon groups linked to carboxyl groups, usually in esterified form, and are important components of lipids such as glycerides, phospholipids and glycolipids. Esterified fatty acids are hydrolyzed to obtain free fatty acids, which are intermediate products in the process of fat metabolism, and they serve as both the donor of lipid structural components of cell membranes and prostaglandin synthesis, as well as one of the important energy supply substances in the human body. Free fatty acids can be divided into short-chain fatty acids (≤ 6 carbons), (SCFAs), medium-chain fatty acids (7~12 carbons) (MCFAs) and long-chain fatty acids (≥12 carbons) (LCFAs) according to their different chain lengths. According to their unsaturation, it can be divided into monounsaturated fatty acids (MUFAs) and polyunsaturated fatty acids (PUFAs). According to the position of the first double bond from the carbon atoms at both ends, it is divided into n-3, n-6, n-7 and n-9 series of unsaturated fatty acids. Long-chain polyunsaturated fatty acids (LC-PUFAs) are a class of fatty acids that have been widely studied and concerned, and n-3 and n-6 PUFAs are the most important (1). Among them, n-6 PUFAs mainly include linoleic acid (LA) and arachidonic acid (ARA or AA), etc., and n-3 PUFAs include alpha-linolenic acid (ALA), docosahexaenoic acid (DHA) and eicosapentaenoic acid (EPA)., etc. Lipoxygenase and cyclooxygenase-2 stereoselectively convert the polyunsaturated fatty acids arachidonic acid, eicosapentaenoic acid, docosahexaenoic acid and n-3 docosapentaenoic acid into a large number of oxidized products (2). It has long been demonstrated that lipoxins (LXs) are oxidation products of arachidonic acid (AA) in the eicosanoids family (3). Biosynthetic pathway studies have shown that different families of endogenous products are formed during the regression phase of acute inflammation. These products have been named specifically lysolytic mediators because of their specific function in the inflammatory resolution circuit, which can enhance the return of inflamed and injured tissues to homeostasis (2). In summary, Resolvins D and E, maresins, and lipoxins constitute important classes of specialized proresolving mediators, and the former three are biosynthesized from n-3 fatty acids while the origin of the last one is n-6 fatty acids (4, 5).

1.2 Biological Functions of Polyunsaturated Fatty Acids

PUFAs are closely related to the normal physiological functions of the human body, with functions such as enhancing memory, preventing cancer, resisting aging, reducing blood lipids and blood pressure, anti-thrombosis, preventing platelet aggregation, reducing levels of low-density lipoproteins in the blood and slowing arteriosclerosis. They have good preventive and therapeutic effects on diseases such as heart disease, arthritis, and diabetes. Research has shown that low doses of AT-RvD1 and RvD2 can significantly improve the disease activity index, weight loss, colon damage, and polymorphonuclear cell infiltration (6). Serhan et al. discovered a new pro-lipid dissolution mediator, which includes the lipoxin, resolvin, protectin, and maresin families, collectively called specialized pro-resolving mediators (7). The synthetic samples of these mediators have a powerful biological activity when given in the body. In animal experiments, the mediator triggers an anti-inflammatory and new pro-dissolving property, and enhances the clearance rate of microbes. Protectins and maresins are two structurally different families. NPD1/PD1 can reduce neuroinflammation, stimulate resolution, and relieve pain; MaR1 can stimulate tissue regeneration and resolution, has anti-inflammatory effects, and can reduce pain, protect organs, and reshape tissue (8). RvD1, RvD2, and MaR1 can inhibit the release of pro-inflammatory cytokines while increasing the production of anti-inflammatory cytokines (9); MaR1 can induce the formation of platelet-lytic substances in human blood, preventing the occurrence of cardiovascular diseases (10); Lipoxin A4 is often synthesized by transcellular pathways in inflammatory responses, can produce potent anti-inflammatory effects, and can affect the onset and development of diabetes by regulating the release and expression of various substances in the body (11). Recent research shows that lipoxins, resolvins, protectins, and maresins regulate endogenous decomposition processes by limiting further infiltration of neutrophil tissue and stimulating local immune cells (such as macrophages) mediated apoptosis polymorphonuclear neutrophils, cell debris, and microbial clearance as well as downregulation of arachidonic acid/cytokine production (12). In summary, Resolvins D and E, maresins, and lipoxins compounds exhibit intrinsic biological functions and play important physiological roles in inflammatory responses such as anti-inflammatory, proresolving, protective functions, etc. (5, 13, 14). Therefore, the quantitative or qualitative analysis of Resolvins D and E, maresins, and lipoxins is crucial for the diagnosis or progression monitoring of human diseases.

2. Progress in the Analysis and Research of Polyunsaturated Fatty Acids

2.1. Structural characteristics of Polyunsaturated Fatty Acids

PUFAs are straight-chain fatty acids containing two or more double bonds and 16-22 carbon atoms. In nature, these double bonds are usually in the cis format, except some in ruminant milk, meat and hydrogenated oils are in the trans (15). Resolvins D and E, maresins and lipoxins exist in a diverse array of structures that include the number of carbons (C20 or C22), hydroxyl groups (two or three), carbon-carbon double bonds (four to six), and their configurations. They contain allylic vicinal diol groups.

2.2. Methods for Fatty Acids Detection

The traditional detection methods for free fatty acids mainly include Gas Chromatography-Mass Spectrometry (GC-MS) (16, 17) and Liquid Chromatography-Mass Spectrometry (LC-MS) (18, 19). The content of free fatty acids is extremely low in organisms and oils and their structure lacks easily ionizable functional groups, resulting in low sensitivity in mass spectrometric analysis. The Stable Isotope Dilution LC-MS method (ID LC-MS/MS) uses test substances labeled with stable isotopes (like ^{13}C, ^{15}N, ^{2}H etc.) as internal standards (diluents), to obtain reliable absolute lipid quantification results, through precise mass spectrometric detection of isotope abundance and accurate addition of diluents (20, 21). However, the synthesis of isotopic internal standards is difficult and expensive, and the commercial products are insufficient to obtain a one-to-one internal standard for analytes, limiting the widespread use of this method.

Chemical derivatization (22) is a method that reacts a compound under test with a derivatization reagent with specific groups to generate a derivatization product that meets the requirements and then indirectly determines the content of the test substance by detecting the amount of the derivatization product. After chemical derivatization, the detection characteristics of the test substance can be changed, increasing its response to the detector and generating stable derivative products to improve the instability of the test substance. Derivatization techniques can improve ionization efficiency, reduce ion suppression in complex sample analysis, and thus enhance the sensitivity and selectivity of electrospray mass spectrometry analysis. Derivatization techniques are suitable for accurate and relative quantitative analysis of metabolites with target functional groups in actual samples.

In recent years, isotope-coded derivatization (ICD) technology performs isotopic labeling on the specific functional groups of the target object through derivatization

reactions. Combined with LC-MS, it can specifically analyze molecules with similar reaction characteristics (23). This technology not only solves the problem of insufficient sensitivity in the analysis of complex matrix biological samples but also provides a solution for the difficulty in obtaining isotopic internal standards in quantitative analysis and has been widely used in the field of metabolomics. By using this strategy, free fatty acids undergo esterification or acylation reactions with derivatization reagents, and the polarity of the derivatized products is changed, thereby effectively separating using liquid chromatography. At the same time, the readily ionizable functional groups contained in the derivatization reagent can improve the detection sensitivity of the product, thereby effectively improving the mass spectrometry ion response of such substances and laying the foundation for quantitative analysis. N, N-dimethylethylenediamine (DMED) can react with carboxylic compounds to produce derivatives with tertially amine groups, and the derivatives are stable (24). Epoxidized/ dihydroxylated oxidized lipids are important bioactive compounds formed mainly from polyunsaturated fatty acids (PUFA) in reactions catalyzed by cytochrome P450 (CYP 450) enzymes. N, N-dimethylethylenediamine (DMED) and DMED-d4 isotopically labeled carboxyl-containing epoxidized/ dihydroxylated oxidized lipids were used for rapid screening of potential epoxidized/ dihydroxylated oxidized lipids from complex matrices based on a pair of diagnostic ions (25). However, quantification based on LC-MS still faces some challenges, such as signal drift in LC-MS, which may affect the validity of the obtained data and lead to misinterpretation of biological results.

Electrospray Ionization Mass Spectrometry (ESI-MS) is a soft ionization technique, which can not only determine the relative molecular mass of a compound, but also obtain rich fragment structure information. It is widely used in the field of chemistry, especially deserved to be one of the important analytical tools by studying the fragmentation in MS/MS. For example, the rapid identification of Actinomycins has become possible by studying their fragmentation rules in mass spectrometry in the positive-ion mode (26, 27). However, because weak acid in electrospray droplets, which is derived from the mobile phase of LC, can carry many positive charges, it suppresses the formation of analyte carboxylates to be negative ions, and therefore, inhibiting the ionization efficiency of the analyte. Therefore, conversion of carboxylates into cationic compounds through chemical derivatization, followed by analysis in positive-ion mode, could relatively avoid the ion suppression in LC/ESI-MS/MS, which improves the detection sensitivity of ESI-MS.

In Chapter I, I described the novel chemical derivatization using short basic peptides and its analytical property for the analysis of various types of PUFAs in

positive-ion ESI-MS. In Chapter II, I described the novel fragmentation that is characteristic for the PUFAs containing allylic vicinal diols, and established the quantitative analysis for seven types of PUFAs. In Chapter III, I described the protocol for isolation of PUFAs from serum and the result of quantification of PUFAs in human serum using several commercially available specimens.

Chapter I. Development of a Derivatization Method for Analyzing PUFAs with High Sensitivity and Resolution Using UPLC-MS/MS

I.1 Introduction

I.1-1 Detection of polyunsaturated fatty acids

Most PUFAs can be successfully analyzed by negative-ion MS/MS (28, 29), in which various types of fragment ions, such as dehydrated, decarboxylated, and internally cleaved fragments, have been reported. Fragments that are derived from internal cleavage are useful as the diagnostic ions since that are unique for an individual structure (30-32). Despite the versatility of negative-ion MS/MS, the sensitivity of detection is not always satisfactory and is not suitable for small sample sizes. The sensitivity has been reported to be 10-5,000 times less than that for PUFAs that are derivatized with cationic compounds (33). This is partly because the terminal carboxylate group, which is the only charged site on the molecule, is not completely ionized in the solvent system used for LC, which normally has an acidic pH when the reverse-phase mode of separation is used, resulting in a significant decrease in ion production. It becomes more serious when a sample is prepared from biological or clinical resources such as serum, since the ionization further suffers from matrix effects (34). To put the MS/MS analysis to practical use for such bio-samples, they are derivatized using a cationic compound which enables their detection with a much higher sensitivity in the positive-ion mode MS (33, 35-37). Despite the fact that the method involves a simple sample treatment and allows for the higher sensitivity detection described above, difficulties are often encountered in characterizing each PUFA molecule. This can be attributed not only to the presence of a variety of isomeric structures in each class of PUFAs but also to the fragmentation in MS/MS, which is highly biased toward dehydration on the multiple hydroxyl groups in the molecule or to the degradation of the derivatizing moiety. This becomes an issue when a bio-sample, such as serum, is being analyzed by a multiple-reaction monitoring (MRM) method in LC-MS/MS, which often results in the ambiguous identification of PUFAs, because of the presence of various contaminants which could produce numerous unknown peaks in an MRM chromatogram that can frequently overlap with the target compound. Therefore, exploring the characteristic fragment ions of a certain type of a component in multiple-reaction monitoring (MRM) method

in LC-MS/MS based on its structural feature is of great significance for the reliable identification.

I.1-2 Separation of polyunsaturated fatty acids

As mentioned above, derivatizing agents can detect polyunsaturated fatty acids in the positive-ion mode of LC-MS with high sensitivity (35). However, since these derivatized PUFAs give fragment ions derived primarily from dehydration or degradation of the derivatizing agent's portion of the molecule, so the fragment ion masses are identical among many isomers, making identification difficult. Although current UPLC is capable of separating complex mixtures, it is still difficult to successfully separate these PUFAs. For example, hydroxyeicosatetraenoic acids (HETEs) (Figure 1.) are a series of eicosanoids, and hydroxy docosahexaenoic acids (HDoHEs, HDHAs) (Figure 2.) are metabolites of DHA, which have the same molecular formula and similar structures in each class, differing only in the position of the single hydroxyl group.

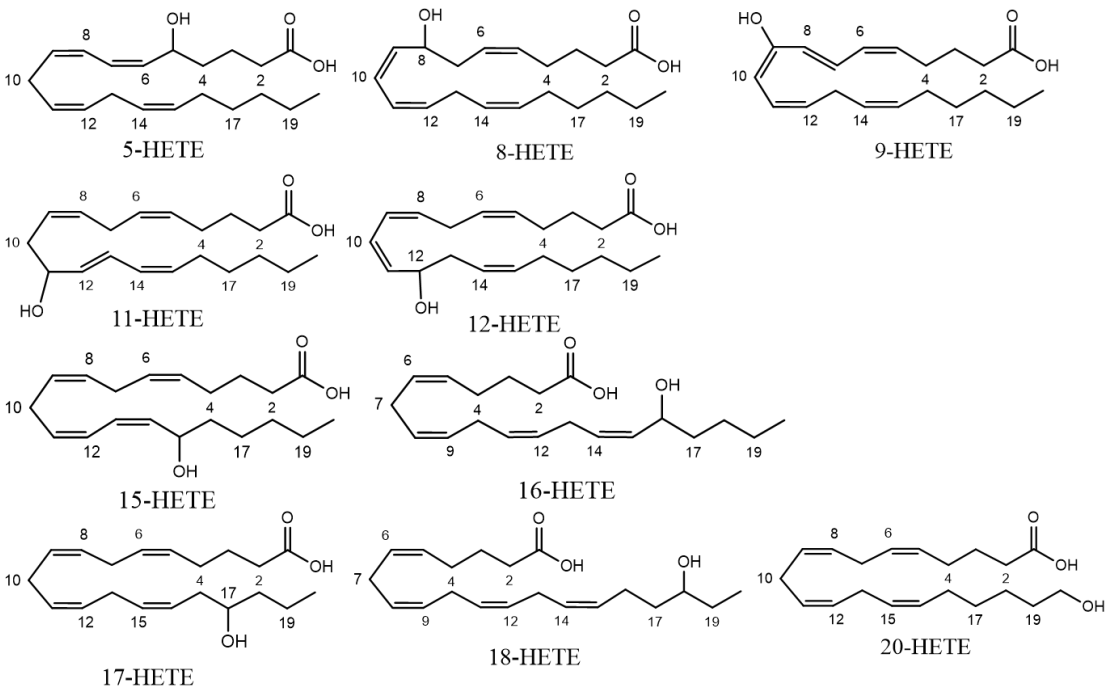

Figure 1. Structures of hydroxyeicosatetraenoic acids (HETEs). The chiral structure of their hydroxyl groups is naturally sinister (S) configuration.

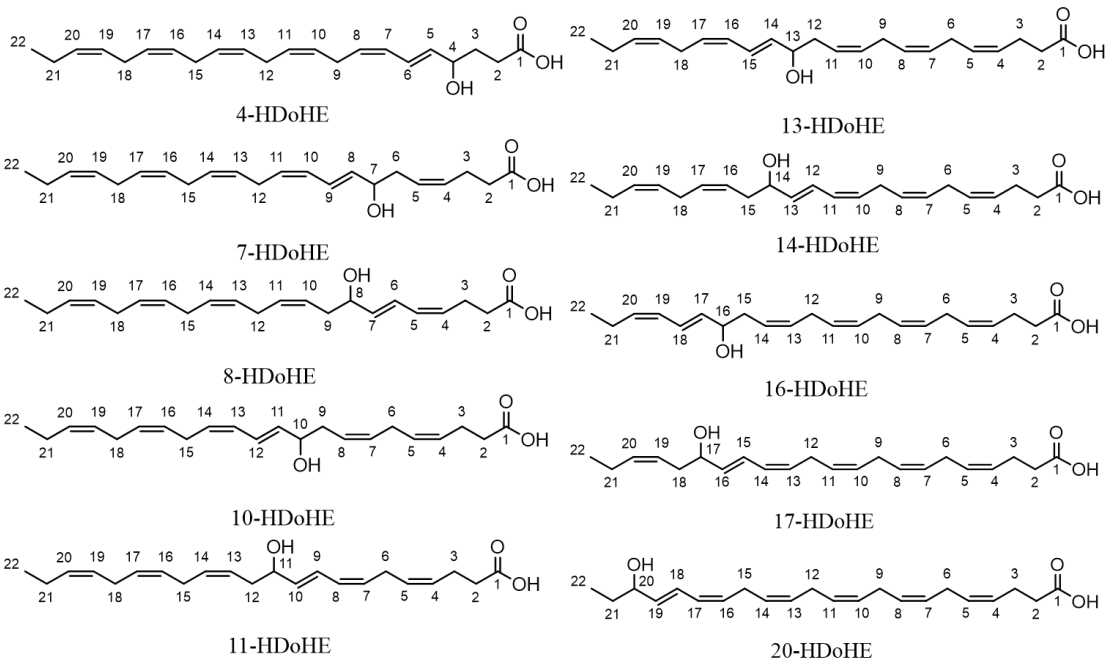

Figure 2. Structures of hydroxy docosahexaenoic acid (HDoHEs, HDHAs). The chiral structure of their hydroxyl groups is naturally sinister (S) configuration.

Because of their similar chemical properties, their elution characteristics are also similar in reversed-phase LC. However, the different positions of the hydroxyl groups create a unique hydrophobicity in the molecule that allows separation by reversed-phase LC. Especially, each of HETEs/HDoHEs classes has the same molecular formula and exhibit extremely similar hydrophobicity, the separation and identification of which have been challenging task.

I.1-3 Use of a peptide as the derivatizing agent

In order to solve the above issue on separation of polyunsaturated fatty acids, a short peptide has been newly designed as a derivatization agent. The method is advantageous in the following points:

1) Fatty acids can be easily attached to the N terminus of a peptide. Peptides are molecules that can be freely designed whose molecular weight and hydrophobicity can be edited. Especially, some of the amino acids are highly responsive in positive-ion mode in MS.
2) The separation of the products can also be modulated by amino acid sequence and length of the peptide, based on hydrophobicity, charge, and fragmentation efficiency (see below).
3) The fragmentation efficiency, which is important for the detection sensitivity in MRM measurement, could be optimized by amino acid sequence.

4) Since any number and kinds of isotopes (^{13}C, ^{15}N) can be incorporated into the peptide, the internal standard with isotopic labeling are readily prepared.
5) To achieve efficient ionization in positive-ion mode of MS, the peptide contains basic amino acid(s) and C-terminally amidated, which, as the result, predominantly gives $[M+2H]^{2+}$ ion. The peptide sequence is designed to be simple and short, resulting in easy and low-cost preparation. Note that a Pro is embedded in the sequence so as to achieve efficient fragmentation at the imide linkage, which is known to be well fragmented upon collision-induced dissociation (CID). (Scheme 1.) In addition, Pro-containing peptide gives an intense immonium ion at m/z 70, which is also produced from Arg-containing peptide, thus making the ion intensity very high (Scheme 2.), which was, therefore, used as the MRM transition (see Table 1.). Since HETEs and HDoHs are relatively hydrophobic, the peptide portion shall be hydrophilic and make the PUFA-conjugates well separable in reverse-phase HPLC. Based on several lines of the considerations described above, three kinds of peptides were prepared and used for the PUFA derivatization. Each of them contains just three kinds of amino acids and has different hydrophobicity: in descending order of hydrophobicity, they are RPFFFR, RPFR, and RPGGGGGGR.

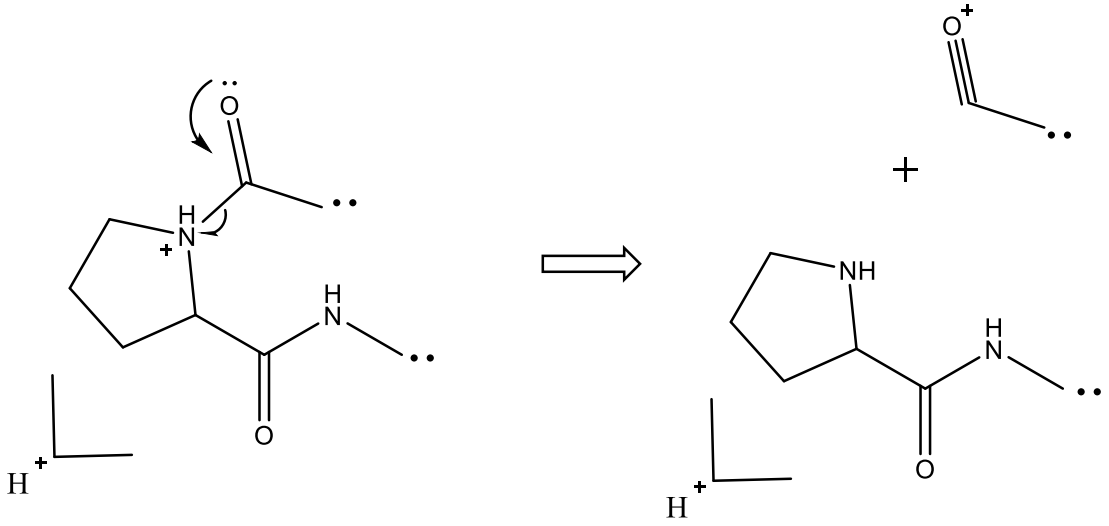

Scheme 1. Fragmentation at the imide linkage, which is known to be well fragmented upon collision-induced dissociation (CID).

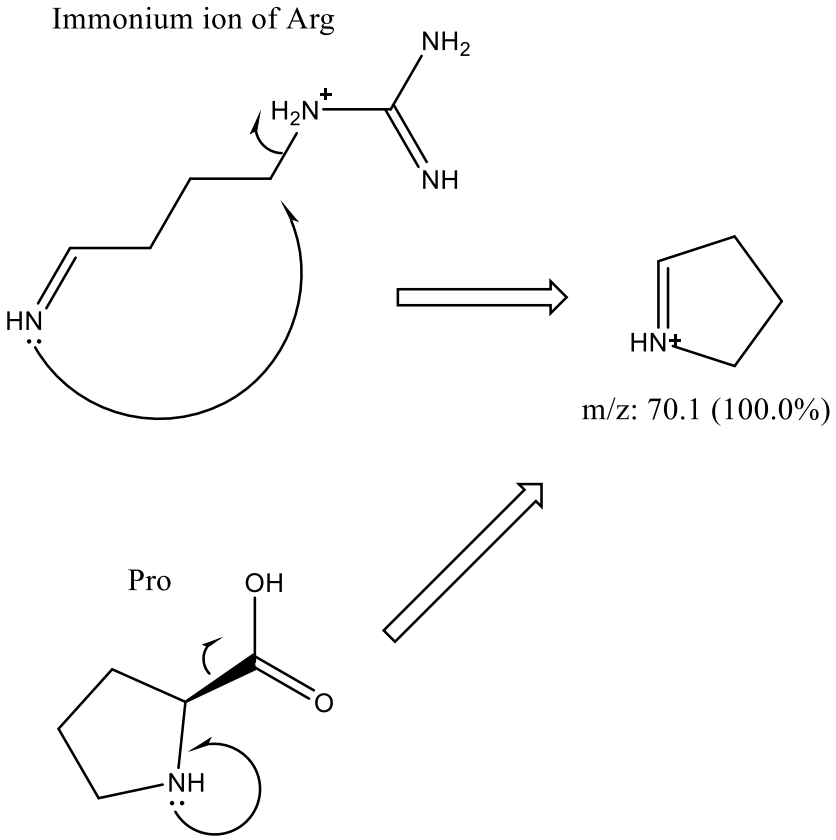

Scheme 2 Immonium ion at m/z 70, which is produced from both Pro-containing peptide and Arg-containing peptide.

I.2 Materials and Methods

I.2-1 Chemicals

HPLC grade Methanol (MeOH), acetonitrile (ACN) and Trifluoroacetic acid (TFA), Reagent special grade N, N-diisopropylethylamine (DIEA) and dimethylformamide (DMF) were purchased from Sigma-Aldrich Co. LLC (St. Louis, MO). 1-[Bis (dimethylamino) methylene]-1H-benzotriazolium-3-Oxide Hexafluorophosphate (HBTU) from Tokyo Chemical Industry Co., Ltd. (Tokyo, Japan). Rink Amide MBHA resin was purchased from Merck KGaA (Darmstadt, Germany). Fmoc-Arg(Pbf)-OH, Fmoc-Pro-OH, Fmoc-Gly-OH and Fmoc-Phe-OH were purchased from PEPTIDE INSTITUTE, INC. (Osaka, Japan). L-PROLINE-N-FMOC ($^{13}C_5$, 99%; ^{15}N, 99%) was obtained from Cambridge Isotope Laboratories, Inc. (Tewksbury, MA). 5-HETE, 8-HETE, 9-HETE, 11-HETE, 12-HETE, 15-HETE, 16-HETE, 17-HETE, 18-HETE, 4-HDoHE, 8-HDoHE, 10-HDoHE, 13-HDoHE, 14-HDoHE, 17-HDoHE, 20-HDoHE were supplied by Cayman Chemical Co. (Ann Arbor, MI). HPLC grade formic acid (FA) and Reagent special grade Pyridine was obtained from FUJIFILM Wako Pure

Chemical Corporation (Osaka, Japan). Ultrapure water was prepared using a puric ω (Organo, Co., Tokyo, Japan). The HF Bond Elut C18 (1 ml, 50 mg) was purchased from Agilent Technologies, Inc. (Santa Clara, CA).

I.2-2 Human sera and ethical approval

Samples of human sera (582-male (25 years old [y.o.]), 594-female (25 y.o.)) without personally identifiable information were purchased from BioIVT (Hicksville, NY). This study was approved by the Ethics Committee of the Institute for Protein Research, Osaka University (No. 2021-1-1). Human studies abided by the Declaration of Helsinki principles.

I.2-3 Preparation of designed peptides

Arg-Pro-Phe -Arg (RPFR), Arg-Pro-Gly-Gly-Gly-Arg (RPGGGR), Arg-Pro-Gly-Gly-Gly- Gly-Gly- Gly-Arg (RPGGGGGGR) and isotope-labeled RP*FR are synthesized by using normal Fmoc solid-phase peptide synthesis method.
P*: Proline ($^{13}C_5$, 99%; ^{15}N, 99%)

I.2-4 Preparation of peptide-derivatized PUFAs

HETEs and HDoHEs were derivatized by reaction with peptide or labeled peptide according to the condensation reaction stage of Fmoc solid phase synthesis. HETEs and HDoHEs in ethanol (0.1ng/μL) were stored at -30 ℃. 40 μL of each stock solution were dried under vacuum and then mixed with 10μl peptide (0.5 M in DMF) and 10 μl of mixture of DIEA (1.2 M in DMF) and HBTU (0.65 M in DMF), promptly purged with argon gas, vortexed for 1 min, and allowed to stand at room temperature for 120 min. Each reaction mixture was diluted with 15% ACN and directly applied to ultra-performance liquid chromatography/ESI-MS/MS for automatic optimization and acquiring the product ion spectra and MRM chromatograms.

The PUFAs were isolated from serum according to a previously reported method with minor modifications (17, 18). Twenty microliters of aliquots from a healthy volunteer aged 25 (see above) was mixed with 100 μL of a 90% ACN/10% MeOH solution containing 0.01 mM 2,6-di-tert-butyl-4-methylphenol, vortexed, allowed to stand at 4℃ for 30 min, and then centrifuged for 15 min at 12,000 rpm. The supernatant was diluted eight times with ultrapure water and then loaded on a Bond Elut C18 column (50 mg) that had been washed with 1 mL of aqueous 70% ACN/0.3% FA and equilibrated with 2 ml of aqueous 5% ACN/0.3% FA. After washing the column three times with 1 mL of 5% ACN/0.3% FA, the PUFAs were eluted with 800 μL of aqueous 70% ACN/0.3% FA. The eluates were evaporated to dryness, derivatized with peptide

as above, and subjected to LC-MS/MS for the MRM analysis (see below).

I.2-5 Liquid chromatography-mass spectrometry

The LC-MS/MS analysis was performed using an Agilent 1290 Infinity II and 6470 triple quadrupole MS, consisting of Q1 (MS1), Q2 (collision-induced dissociation [CID] area), and Q3 (MS2), equipped with an ESI ion source (Agilent Technologies, Inc. Santa Clara, CA). Chromatographic separation was achieved with an Agilent Eclipse Plus C18 RRHD 2.1×100 mm, 1.8 μm column (Agilent Technologies, Inc.), the inlet of which was connected to a heat exchanger (ultralow dispersion) (Agilent Technologies, Inc.), which was maintained at 40 ℃ and connected to an InfinityLab Quick Change inline filter (Agilent Technologies, Inc.). The mobile phase consisted of solvent A (0.3% FA in ultrapure water) and solvent B (0.3% FA in 100% ACN). The elution gradient of single PUFAs was: 30.0-40.0% B (0-5.00 min); 40.0-60.0% B (5.00-10.00 min); 60.0-80.0% B (10.00-10.65 min); 80.0% B (10.65-11.20 min); 80.0-30.0% B (11.20-11.21 min); 30.0% B (11.21-12.50 min).; The elution gradient of serum separation test was: 20.0-80.0% B (0-15.00 min);80.0% B (15.00-16.00 min); 80.0-20.0% B (16.00-16.01 min); 20.0% B (16.01-18.00 min). The elution gradient that optimized for serum PUFAs detection was: 25.0% B (0-0.50 min); 25.0-36.0% B (0.50-1.00 min); 36.0-38.0% B (1.00-3.00 min); 38.0-42.0% B (3.00-5.00 min); 42.0-47.0% B (5.00-10.00 min); 47.0-80.0% B (10.00-11.00 min);80.0-90.0% B (11.00-13.00 min); 90.0-25.0% B (13.00-13.01 min); 25.0% B (13.01-15.00 min). The injection volume was 20 μl for serum sample. The MRM mode was used for detecting the derivatized PUFAs by using the transitions, pairs of m/z values for the precursor and fragment ions, that are listed in (Table 1.), including 2 kinds of fragment ions of each peptide-PUFAs that are derived from peptide-degraded forms. The ion transmission windows of Q1 and Q3 were set as “unit” and “unit,” respectively, where “unit” allows ions with a window of 0.75 Da to pass.

The collision energy voltages were set at 21 or 55 eV and were optimized for each analyte (see Table 1.). The fragmentor voltage, which was intermediate between the capillary exit and the skimmer, was fixed at 150 V. The ESI source parameters were set as follows: capillary voltage of -4500 V in the positive-ion mode, nebulizer (N_2) gas pressure of 30 psi, drying gas (N_2) temperature and flow rate of 240℃ and 13 L·min-1, respectively, and a sheath gas temperature of 250 ℃ was used. Data were acquired using an Agilent MassHunter Acquisition system.

Table 1. MRM transitions and parameters used for the HETEs and HDoHEs derivatized with peptides.

Analyte	Precursor Ion m/z (MH^+)	Fragmentor voltage	Product Ion m/z	Product ion form	CE voltage /eV
HETE-RPFR	438.8	150	70.1	$[C_4H_8N]^+$	55
	438.8	150	418.3	$[C_{20}H_{30}N_6O_4]^+$	21
HETE-RPFFFR	585.8	150	70.1	$[C_4H_8N]^+$	55
	585.8	150	712.7	$[C_{38}H_{48}N_8O_6]^+$	21
HETE-RPGGGGGGR	536.4	150	70.1	$[C_4H_8N]^+$	55
	536.4	150	613.5	$[C_{23}H_{39}N_{11}O_9]^+$	21
HETE-labeled RPFR	441.8	150	75.1	$[^{13}C_4H_8{}^{15}N]^+$	55
	441.8	150	424.3	$[^{13}C_5{}^{12}C_{15}H_{30}{}^{15}N{}^{14}N_4O_4]^+$	21
HDoHE-RPFR	450.8	150	70.1	$[C_4H_8N]^+$	55
	450.8	150	418.3	$[C_{20}H_{30}N_6O_4]^+$	21
HDoHE-RPFFFR	597.8	150	70.1	$[C_4H_8N]^+$	55
	597.8	150	712.7	$[C_{38}H_{48}N_8O_6]^+$	21
HDoHE-RPGGGGGGR	548.3	150	70.1	$[C_4H_8N]^+$	55
	548.3	150	613.5	$[C_{23}H_{39}N_{11}O_9]^+$	21
HDoHE -labeled RPFR	453.8	150	75.1	$[^{13}C_4H_8{}^{15}N]^+$	55
	453.8	150	424.3	$[^{13}C_5{}^{12}C_{15}H_{30}{}^{15}N{}^{14}N_4O_4]^+$	21

I.3 Results and discussion

I.3-1 Fragmentation of peptide-PUFAs

Through preliminary automatic optimization (“MassHunter”, Agilent), the ion at m/z 70 was observed, as the strongest fragment ions, for the PUFAs derivatized with all kinds of peptides, which was derived from Arg or/and Pro (see Scheme. 2). Another prominent fragment ions have been observed for the tested peptides containing Pro, which correspond to the sequence starting from Pro to the C-terminal Arg since the imide bond at the N-terminal side of Pro is relatively amenable to cleavage upon CID. (See Scheme. 1) Both product ions have been used for the diagnostic ions in MRM measurement (see below and Table 1.).

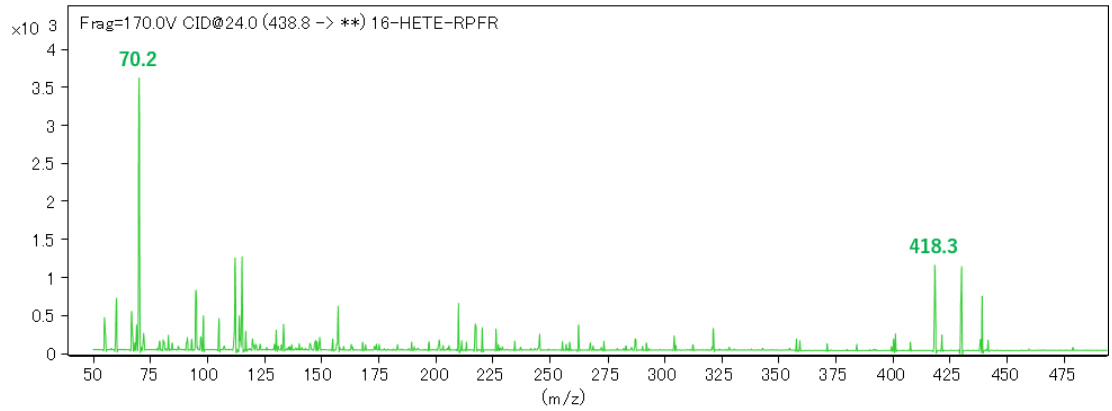

Figure 3 Product ion spectrum of 16-HETE derivatized with RPFR.

I.3-2 Multiple reaction monitoring (MRM) of peptide-PUFAs

Based on the diagnostic ions described in Table I, all HETEs and HDoHEs were examined by MRM. Firstly, each standard was analyzed by MRM to know the retention time, revealing that isomers with proximal hydroxyl groups possess extremely similar properties and are eluted nearby, as in the case of 11-HETE and 12-HETE, and if the two are mixed, they will not be completely separated. (Figure 4.) When two PUFAs are eluted closely, it is impossible to distinguish them in the present analysis, even when the standards are used for comparison.

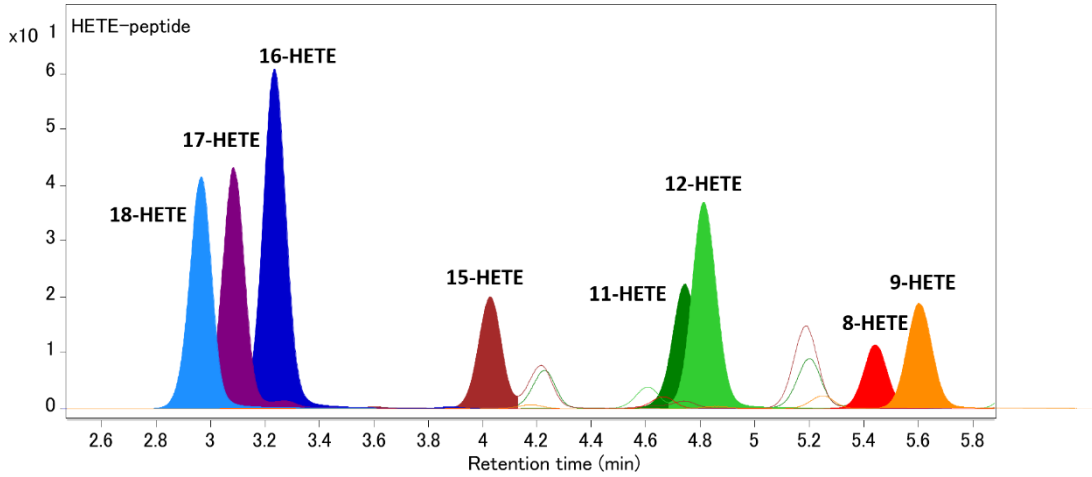

Figure 4 MRM chromatograms of 8-HETE, 9-HETE, 11-HETE, 12-HETE, 15-HETE, 16-HETE, 17-HETE, and 18-HETE derivatized with RPFR.

In order to visualize the difficult separation of isomeric PUFAs in biological samples, serum was used and analyzed directly by MRM. Consistent with expectations, 11-HETE is difficult to separate from 12-HETE. Therefore, three peptides with different hydrophobicity were designed in an attempt to change the hydrophobicity of the derivatized PUFAs and obtain a better separation. The elution gradient was also optimized to allow these three kinds of peptide-PUFAs to appear within the elution time. It turned out that the proximity of elution of similar PUFAs varied with different retention time in the column. When derivatized with the most hydrophilic peptide RPGGGGGGR, some peaks were highly overlapped, whereas, when using the most hydrophobic peptide RPFFFR, the other peaks were overlapped. The RPFR-PUFAs with the intermediate hydrophobicity among the three peptides showed a less overlap in each peak, as the result, all the six PUFAs could be clearly observed. A better separation could be obtained when this elution gradient was further optimized (see Figure 5.). Therefore, the sequence availability of a peptide has proven to have advantages in improving the separation of target substances (peptide-PUFAs) by modulating the hydrophobicity.

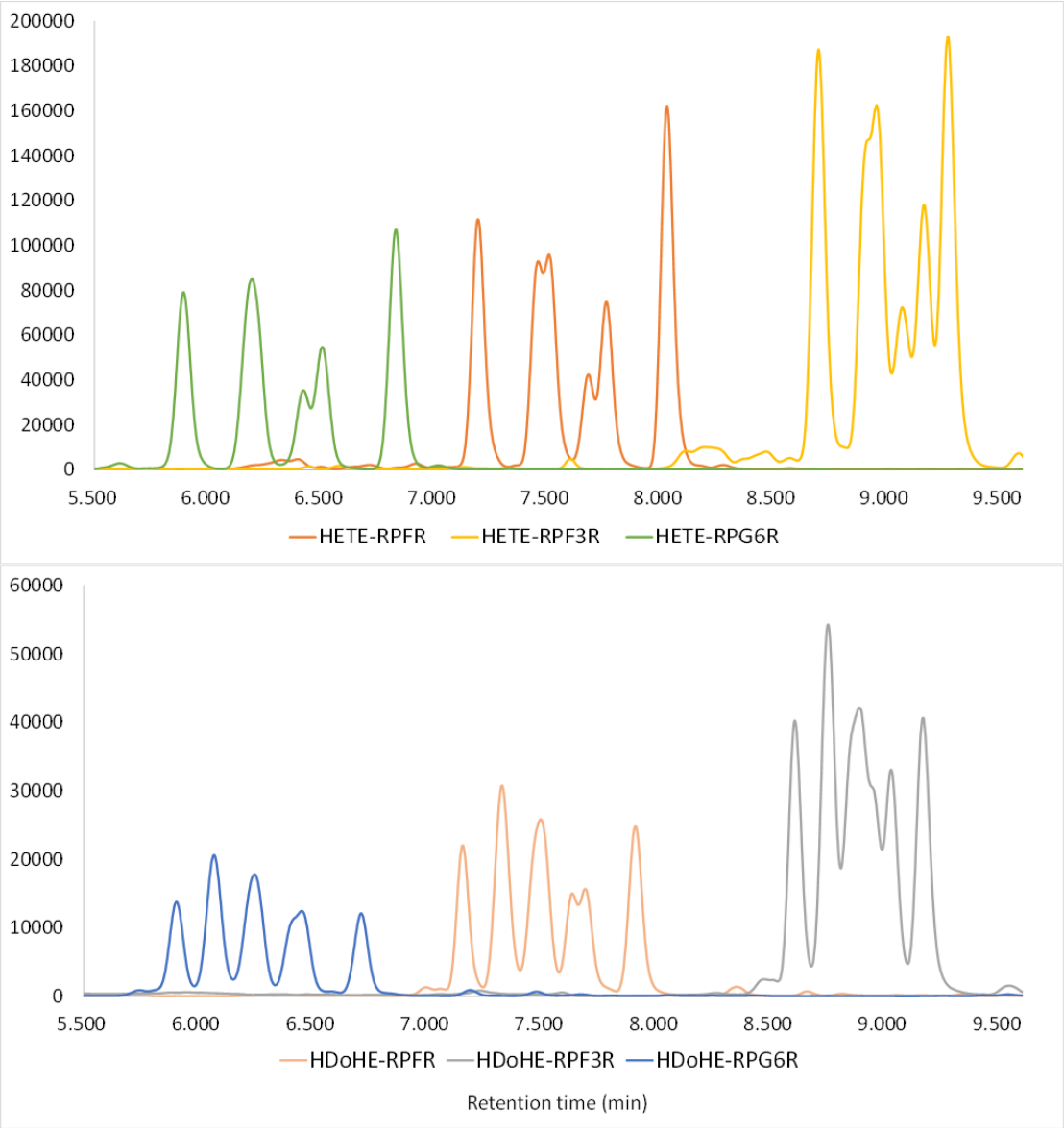

Figure 5. Comparison of MRM chromatograms of HETEs (upper) and HDoHEs (lower) derivatized with RPFR, RPF_3R, and RPG_6R.

I.3-3 Analysis of HETEs and HDoHEs in serum

To determine the types of PUFAs in serum, several isotope-labeled standards of PUFAs were tested. Under the present conditions of separation, however, deuterium-labeled PUFA standards, which are commonly used and commercially available, eluted earlier than the corresponding PUFAs. Note that even though deuterium-labeled compounds are fulfilled and relatively inexpensive, they have distinct chemical properties from the corresponding non-labeled ones owing to the remarkable isotope effect of deuterium. Therefore, commercially available ^{13}C- and ^{15}N-labeled proline (P*), which displays almost no isotope effect, was incorporated into the RPFR. Then, HETEs and HDoHEs were derivatized with RP*FR and spiked into the

serum sample, which has been derivatized with non-labeled RPFR, before analysis. As the result, 15-, 11-, 12-, 8-, 9-, and 5-HETE, and 20-, 14-, 10-, and 8-HDoHE were identified in female serum (Figure 6.).

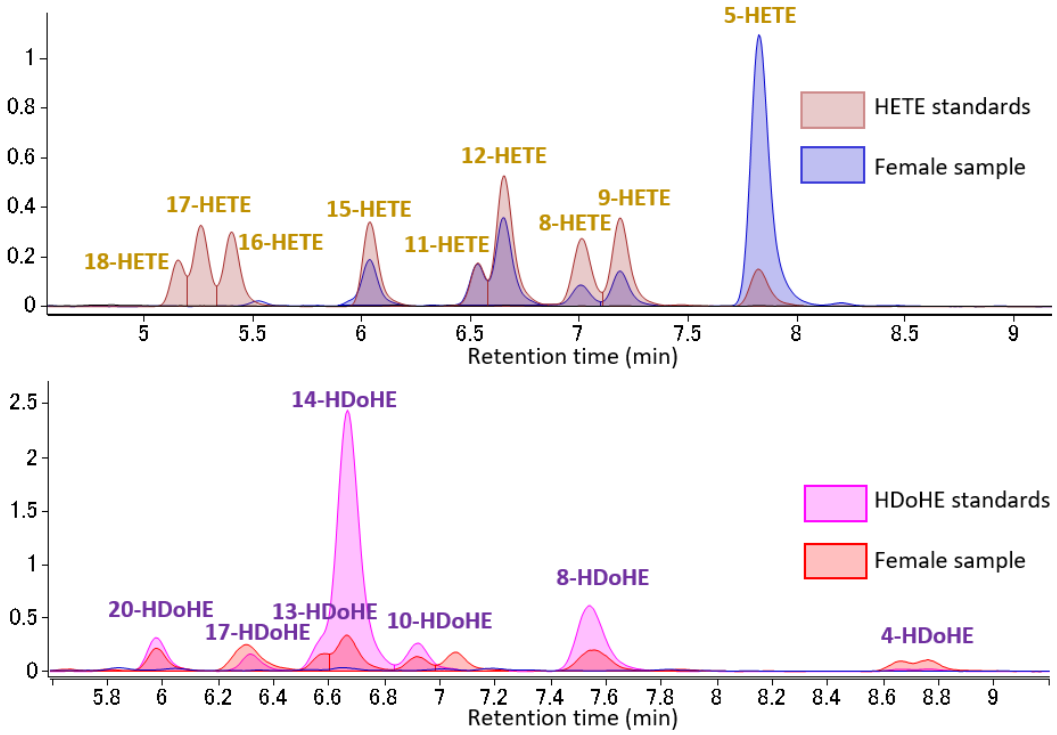

Figure 6. MRM chromatograms of female serum after derivatization using RPFR, overlaid with those of the standard mixtures of HETEs and HDoHEs derivatized with isotope-labeled RP*FR.

Since isotope-labeled peptide can be used as derivatizing agent and were successfully applied for the analysis using internal standards, it was further applied to a comparative analysis between two sample pools. Two different sera were separately derivatized with RPFR and isotope-labeled RP*FR, and then, the same amount of the samples were mixed and applied to MRM measurement. The differences in contents of each PUFA were observed between these individuals (Figure 7.). The result suggested that direct comparison of bio-samples, prepared from different individuals, could be possible by this method. It allows to see promptly the difference in levels of these PUFA between two samples without quantitative analysis of each sample. Each PUFA level might be changed in such as sex, age, or disease, which allows it to be a biomarker for them.

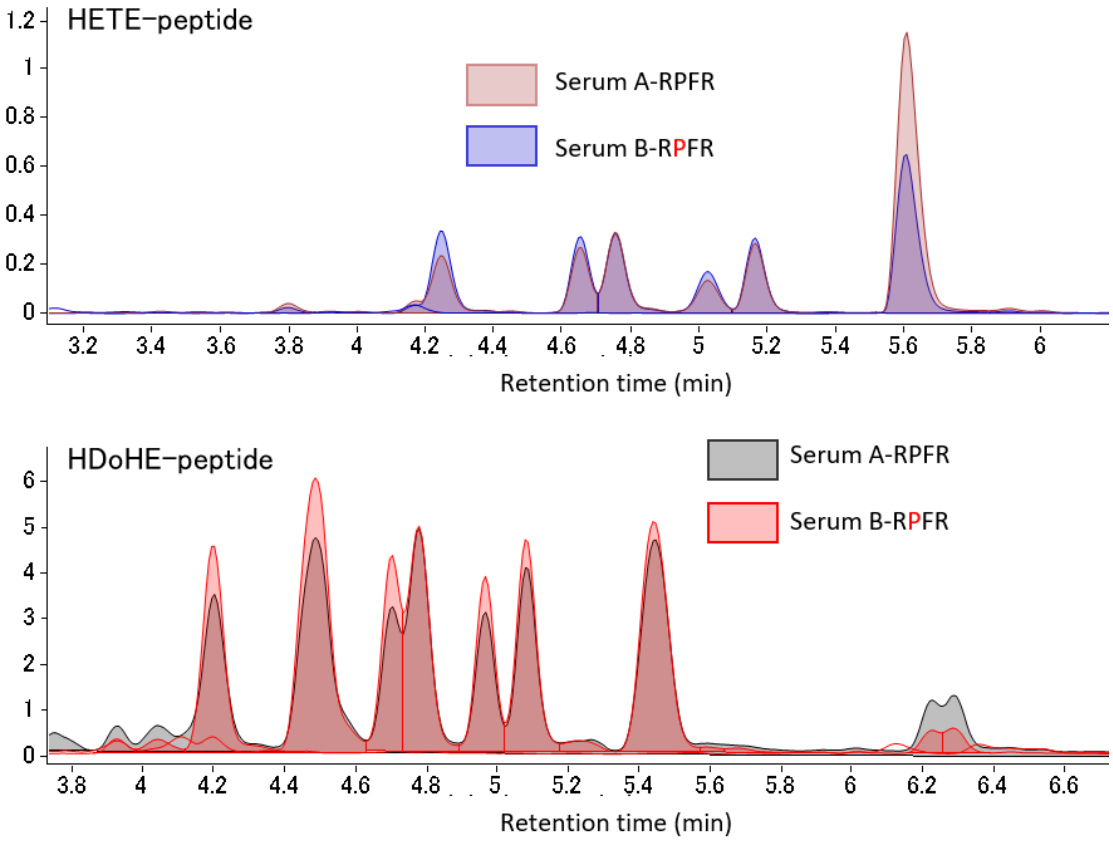

Figure 7. Overlay of the MRM chromatograms obtained for serum A and B after derivatization using RPFR and isotope-labeled RP*FR, respectively.

I.4 Conclusion

A peptide could be used as the derivatizing agent for PUFAs, which allowed editing of its sequence to meet with the hydrophobicity suitable for the separation in reverse-phase LC. Three kinds of peptides were tested, with respect to the separation capability using serum. In case of HETEs and HDoHEs, RPFR-NH_2 gave the best separation in the present reverse-phase UPLC system. Furthermore, the peptide moiety can be easily labeled with a stable isotope, allowing it to be used not only as an internal standard but also for comparative analysis among multiple samples at once.

Chapter II. Characteristic Fragmentation of PUFAs with Allylic Vicinal Diols

II.1 Introduction

Resolvins, maresins, and lipoxins exhibit inherent biological properties, such as anti-inflammatory and pro-resolving responses, playing a crucial role in regulating human T cell responses and improving human immune function (2-4). However, there are currently few research reports on the detection methods for these substances. I report herein on a characteristic fragmentation of PUFAs, derivatized by *N, N*-dimethylethylenediamine (DMED), that contain allylic vicinal diols, namely, resolvin D1 (RvD1), resolvin D2 (RvD2), and resolvin D4 (RvD4); 5S, 6R-lipoxin A4 (LxA4) and 5S, 14R-lipoxin B4 (LxB4); maresin 2 (Mar2), and resolvin E3. They specifically gave either aldehyde (-CH=O) or allylic carbene (-CH=CH-CH:)-terminal fragment ions as the result of breakdown in between the vicinal diol groups.

II.2 Materials and Methods

II.2-1 Chemicals

HPLC grade MeOH, acetonitrile (ACN), dimethylformamide (DMF, Pharmaceutical Secondary Standard grade), 2,6-di-tert-butyl-4-methylphenol (BHT), N,N -Dimethylethylenediamine (DMED), trimethylamine (TEA), and 2-chloro-1-methylpyridinium iodide (CMPI) were purchased from Sigma-Aldrich Co. LLC (St. Louis, MO). RvD1, RvD2, and RvD4; LxA4 and LxB4; maresin 1 and Mar2; 9,10-DiHOME, 12,13-DiHOME, *5S, 6R*-Lipoxin A4-19,19,20,20,20-d5; and Resolvin D1-21,21,22,22,22-d5 were supplied by Cayman Chemical Co. (Ann Arbor, MI). *18S*-Resolvin E3 and *18R*-Resolvin E3 (RvE3R) were prepared as described previously (38, 39). HPLC grade formic acid (FA) was obtained from FUJIFILM Wako Pure Chemical Corporation (Osaka, Japan). Ultrapure water was prepared using a puric ω (Organo, Co., Tokyo, Japan). The HF Bond Elut C18 (1 ml, 50 mg) was purchased from Agilent Technologies, Inc. (Santa Clara, CA).

II.2-2 Human sera and ethical approval.

Samples of human sera (585-male (20 y.o.), 587-male (36 y.o.)) without personally identifiable information were purchased from BioIVT (Hicksville, NY). This study was approved by the Ethics Committee of the Institute for Protein Research, Osaka

University (No. 2021-1-1). Human studies abided by the Declaration of Helsinki principles.

II.2-3 Preparation of DMED-derivatized PUFAs

The PUFAs were derivatized by reaction with DMED according to a previously reported method (35) with minor modifications. Briefly, the PUFAs (10 μg for each in ethanol) were dried under vacuum and re-dissolved in 400 μl Pharmaceutical Secondary Standard DMF and stored at -80 ℃ (stock solution). Four microliters of each stock solution were mixed with 1.5 μl of DMED (300 mM) and 1.5 μl of trimethylamine (150 mM) and then with 1.5 μl of 2-chloro-1-methylpyridinium iodide (75 mM), promptly purged with argon gas, vortexed for 1 min, and allowed to stand at room temperature for 30 min. Each reaction mixture was diluted with DMF and directly applied to ultra performance liquid chromatography/ESI-MS/MS for acquiring the MRM chromatograms (Figure 10.) and product ion spectra (Figure 9).

II.2-4 LC-MS/MS.

The LC-MS/MS analysis was performed using an Agilent 1290 Infinity II and 6470 triple quadrupole mass spectrometer (MS), consisting of Q1 (MS1), Q2 (collision-induced dissociation (CID) area), and Q3 (MS2), equipped with an ESI ion source (Agilent Technologies, Inc. Santa Clara, CA). Chromatographic separation was achieved with an Agilent Eclipse Plus C18 RRHD 2.1x100 mm, 1.8 μm column (Agilent Technologies, Inc.), the inlet of which was connected to a heat exchanger (ultra-low dispersion) (Agilent Technologies, Inc.), which was maintained at 60 °C and connected to an InfinityLab Quick Change inline filter (Agilent Technologies, Inc.). The mobile phase consisted of solvent A (0.3% formic acid in ultrapure water) and solvent B (0.3% formic acid in 20% MeOH and 80% ACN). The elution gradient was: 25.0-28.0 % B (0 to 5.00 min); 28.0-45.0% B (5.00 to 10.00 min); 45.0-80.0% B (10.00 to 11.00 min); 80.0% B (11.00-12.00 min); 80.0-25 % B (12.00 to 12.01 min); 25.0% B (12.01-14.00 min). The injection volume was 20 μL for all samples. The MRM mode was used for detecting the derivatized PUFAs by using the transitions, pairs of m/z values for the precursor and fragment ions, that are listed in Table 2. including those derived from the doubly dehydrated or DMED-degraded forms. The ion-transmission windows of Q1 and Q3 were set as “widest” and “unit”, respectively, where “widest” allows ions with a mass window of 2.5 Da to pass, while “unit” allows ions with a window of 0.75 Da to pass.

The collision energy (CE) voltages were set at 10, 15, or 20 eV, and were optimized for each analyte (see Table 2.). The fragmentor voltage, which was

intermediate between the capillary exit and the skimmer, was fixed at 110 V. The ESI source parameters were set as follows: capillary voltage of -4500 V in the positive ion mode, nebulizer (N_2) gas pressure of 30 psi, drying gas (N_2) temperature and flow rate of 240 ℃ and 13 $L \cdot min^{-1}$, respectively, and a sheath gas temperature of 250 ℃ was used. Product-ion spectra were obtained by injecting 2.5 ng of each of the DMED-derivatized PUFA into the LC-MS/MS which was operated under the same conditions as above. Data were acquired using an Agilent MassHunter Acquisition system, and processed using Agilent MassHunter Quantitive Analysis.

Table 2. MRM transitions and parameters obtained for the authentic PUFAs containing vicinal diols (bold) and their isobaric isomers derivatized with DMED.

Analyte	RT/min	Precursor Ion m/z (MH^+)	Fragmentor voltage	Product Ion m/z	Product ion form	CE voltage /eV
Resolvin D1[a]	7.13	447.3	110	213.2	$[M- C_{15}H_{22}O_2+H]^+$ [b]	14
Resolvin D2[a]	5.92	447.3	110	331.3	$[M- C_6H_{12}O_2+H]^+$ [c]	18
Resolvin D3	6.41	447.3	110	411.3	$[M- 2H_2O+H]^+$ [d]	14
Resolvin D4[a]	8.74	447.3	110	173.3	$[M- C_{18}H_{26}O_2+H]^+$ [b]	10
Resolvin E2	7.89	405.3	110	369.3	$[M- 2H_2O+H]^+$ [d]	15
18*S*-Resolvin E3[a]	8.21	405.3	110	329.3	$[M- C_3H_8O_2+H]^+$ [c]	10
18*R*-Resolvin E3[a]	8.69	405.3	110	329.3	$[M- C_3H_8O_2+H]^+$ [c]	10
Resolvin E4	8.39	405.3	110	369.3	$[M- 2H_2O+H]^+$ [d]	15
Lipoxin A4[a]	7.29	423.3	110	187.3	$[M- C_{15}H_{24}O_2+H]^+$ [b]	10
Lipoxin B4[a]	5.67	423.3	110	305.3	$[M- C_6H_{14}O_2+H]^+$ [c]	15
Maresin 1	9.55	431.3	110	395.2	$[M- 2H_2O+H]^+$ [d]	14
Maresin 2[a]	9.83	431.3	110	275.2	$[M- C_9H_{16}O_2+H]^+$ [c]	14
9,10-DiHOME	9.52	385.3	110	340.3	$[M- C_2H_7N]^+$ [e]	20
12,13-DiHOME	9.09	385.3	110	340.3	$[M- C_2H_7N]^+$ [e]	20

[a] contain allylic vicinal diols.

[b] Aldehyde-terminal ion.

[c] Carben-terminal ion.

[d] Doubly dehydrated ion.

[e] DMED-degraded fragment ion.

II.2-5 Calibration curves and linearity ranges of the PUFAs.

The calibration curve was constructed using the peak height ratios of a compound to IS versus the ratios of concentrations of a compound at seven to nine different levels to the fixed concentration of IS. Based on the detection responses of the PUFAs in the MRM measurement, the concentration ranges for the calibration curves of each PUFA were set. A mixture of six types of PUFAs, except for RvE3R, with the highest concentration (M1) for each was prepared (see Table 3.) using the "stock solution". Note that since RvE3 is not commercially available and the amount on hand was limited, it was separately prepared. Two types of deuterated PUFAs, LxA4-d5 and RvD1-d5, were mixed at concentrations of 5.83 and 2.73 nM, respectively, to prepare the internal standard mixture (IS). Then, 5 μL of M1 and 3 μL of IS was added to the dried residues, which were separately prepared from 200 μL aliquots of serum ("585-male" or "587-male"), as described in **Materials and Methods of Chapter III**, except for the elution with 800 μL of aqueous 5% ACN/0.3% FA. Following the addition of 1.5 μL of DMED (300 mM) and 1.5 μL of TEA (150 mM), 1.5 μL of CMPI (75 mM) was added. The sample was purged with argon, and allowed to stand for 30 min at room temperature to allow the DMED derivatization to reach completion. It is important to note that a matrix such as those prepared from bio-samples turned out to be required to acquire standard curves with good linearity and accuracy. In the present study, the serum eluates, as the matrix, from the HF Bond Elut C18 column (6 mL, 500 mg) with 2%, 5%, and 10% ACN/0.3% FA were examined. Since commercial serum frequently contains considerable amounts of the target PUFAs, which, in turn, significantly affected the calibration, "585-male" or "587-male"-derived serum samples that contained very small amounts of these PUFAs were selected, and their extract with aqueous 5% ACN/0.3% FA was used as a matrix.

M1 was next diluted twice with DMF to make M2, after which 5 μL of M2 was mixed with 3 μL of IS. The sample was then added to the dry serum sample, and derivatized with DMED as described above. This procedure was repeated until M9 or M8 or M7 was prepared. Finally, 12.5 μL of each reaction mixture was diluted twice with H_2O, and a 20 μL portion was then applied to the MRM measurements.

II.3 Results and Discussion

II.3-1 Characteristic fragment ions observed for the PUFAs that contain allylic vicinal diols

Through measurements of various types of PUFAs, it was found that PUFAs that contain allylic vicinal diols (Figure 8.) gave the characteristic fragment ions in their product ion spectra (A, B, D-G, and I in Figure 9), which were derived from the cleavage of the bond between the vicinal diols. In contrast, such ions were not observed at all for their isobaric isomers (C and H in Figure 9) and the PUFAs containing vicinal diols that are not located at the allylic position (e.g. 9, 10-DiHOME (J) and 12, 13-DiHOME (K) in Figure 9). In addition, when the allylic hydroxyl group is located distal to the terminal DMED moiety (RvD1, RvD4, and LxA4), an aldehyde (-CH=O) type of ion was predominantly observed, whereas, in the case where the hydroxyl group is located proximal to the DMED (RvD2, RvE3, LxB4, and Mar2), allylic carbene (-CH=CH-CH:) fragments were the major products, both of which arose from specific cleavage between the vicinal diols (Scheme. 3). Such characteristic fragmentation could be accounted for by the propensity of the allylic carbene, adjacent to the vicinal diols, being preferably formed upon CID in MS/MS based on its stability. The observation of either of these two types of fragment ions are indicative of the location of the cationic DMED moiety, on which a proton was largely localized in the positive-ion ESI-MS/MS (see Figure 9.). It should also be noted that the aldehyde-type of ions were relatively abundant compared with the carbene-type ions (Figure 10.). Since, in general, a carbene is more reactive than an aldehyde, the lifetime in a CID area (Q2) should be relatively short.

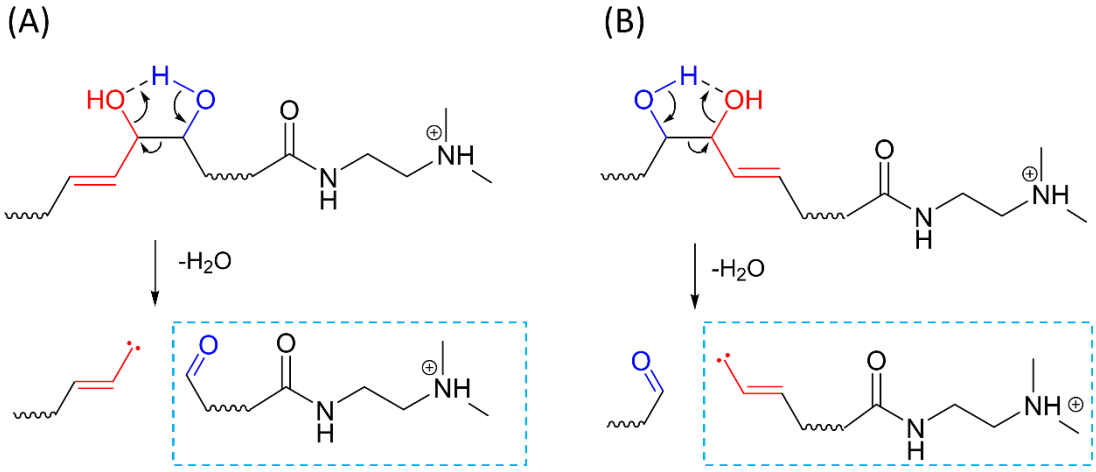

Scheme 3. Fragmentation at allylic vicinal diols observed for polyunsaturated fatty acids. The allyl hydroxyl group is colored in red; the adjoining hydroxyl is in blue. Based on likelihood of an allyl carbene being formed upon CID in ESI-MS/MS, PUFAs (RvD1, RvD4, and LxA4) with an allylic hydroxyl group located distal to the terminal DMED moiety, the aldehyde form was predominantly observed (A), those located proximal to the DMED moiety (RvD2, RvE3, LxB4, and Mar2), the allylic carbene form was observed (B). Protons could also be transferred to the hydroxyl group from the DMED moiety.

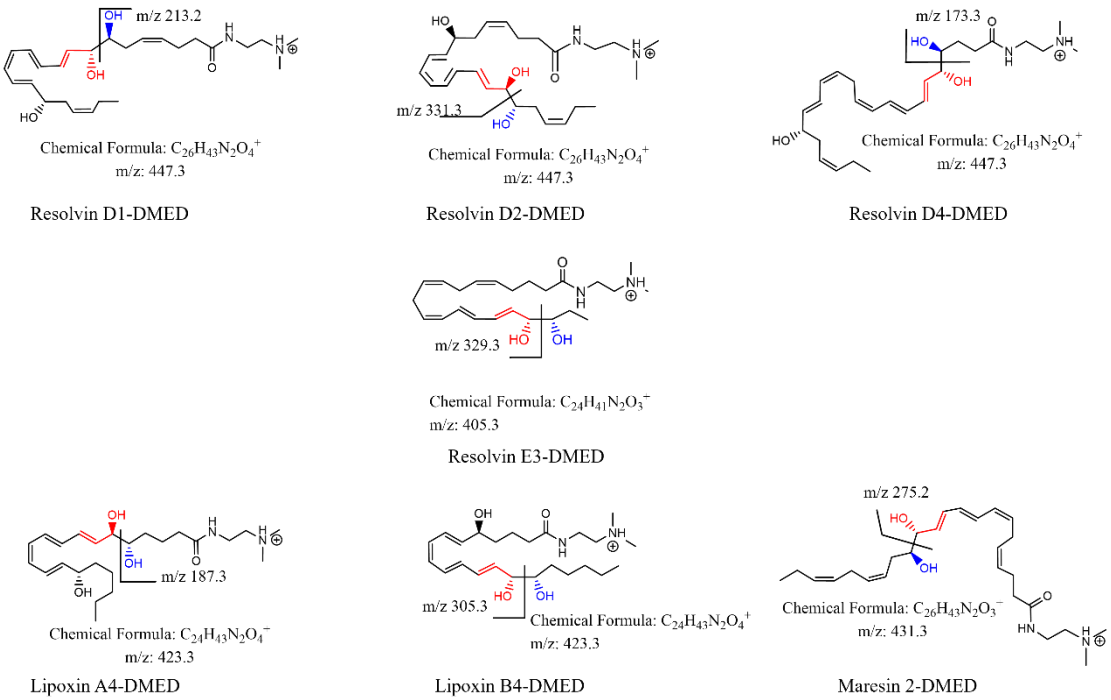

Figure 8. Polyunsaturated fatty acids that contain allylic vicinal diols. The m/z values of the characteristic fragment ions, observed in the positive-ion ESI-MS/MS, are indicated in the structures (see Figure 9.). The allyl hydroxyl group is colored in red; the adjoining hydroxyl group is in blue.

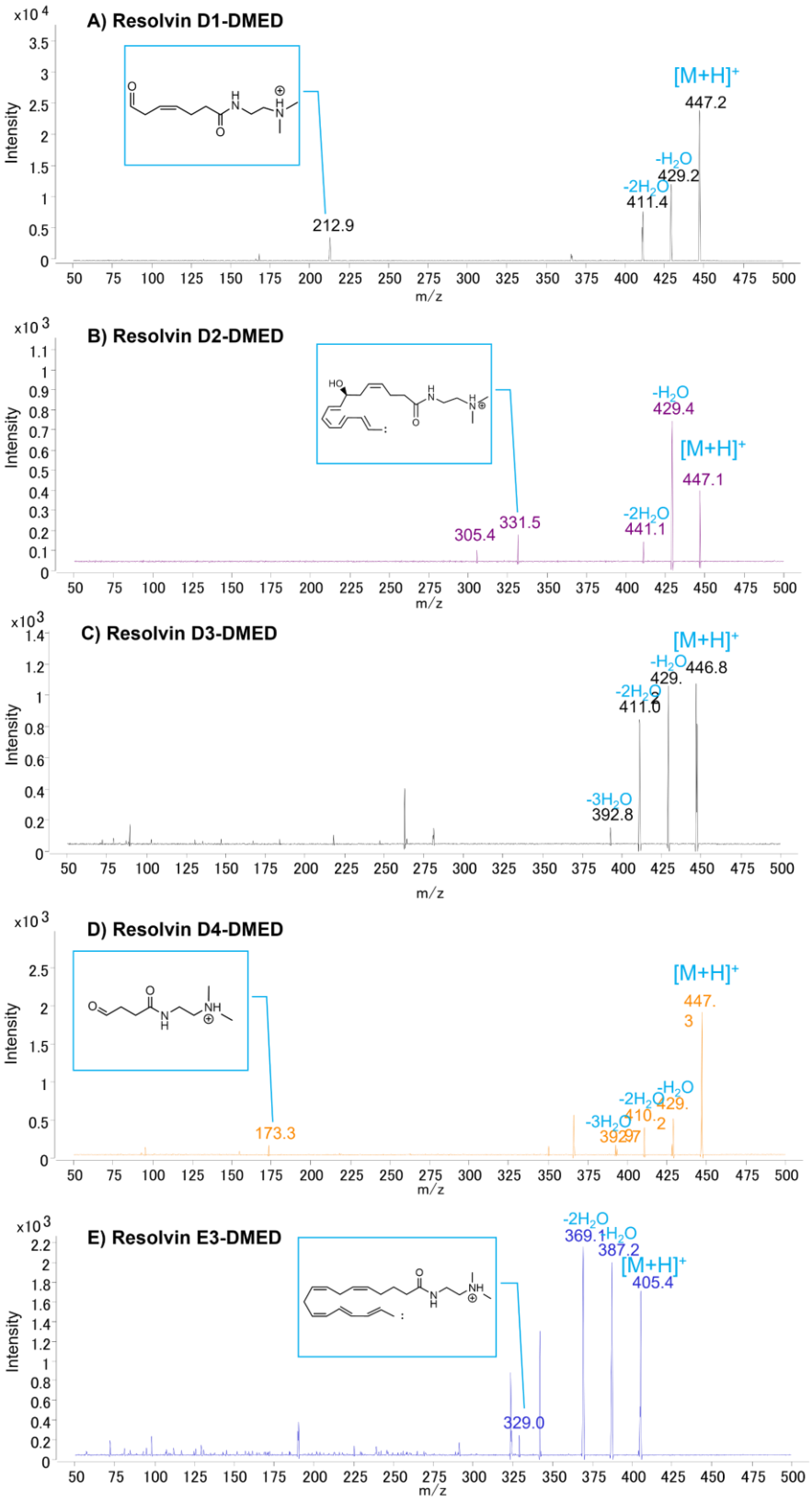
A) Resolvin D1-DMED
x10 4
Intensity
[M+H]+
447.2
-H2O
429.2
-2H2O
411.4
212.9
m/z
B) Resolvin D2-DMED
x10 3
-H2O
429.4
[M+H]+
447.1
-2H2O
441.1
305.4
331.5
C) Resolvin D3-DMED
[M+H]+
446.8
-2H2O
411.0
-3H2O
392.8
D) Resolvin D4-DMED
[M+H]+
447.3
-H2O
-2H2O
-3H2O
173.3
E) Resolvin E3-DMED
-2H2O
369.1
-H2O
387.2
[M+H]+
405.4
329.0

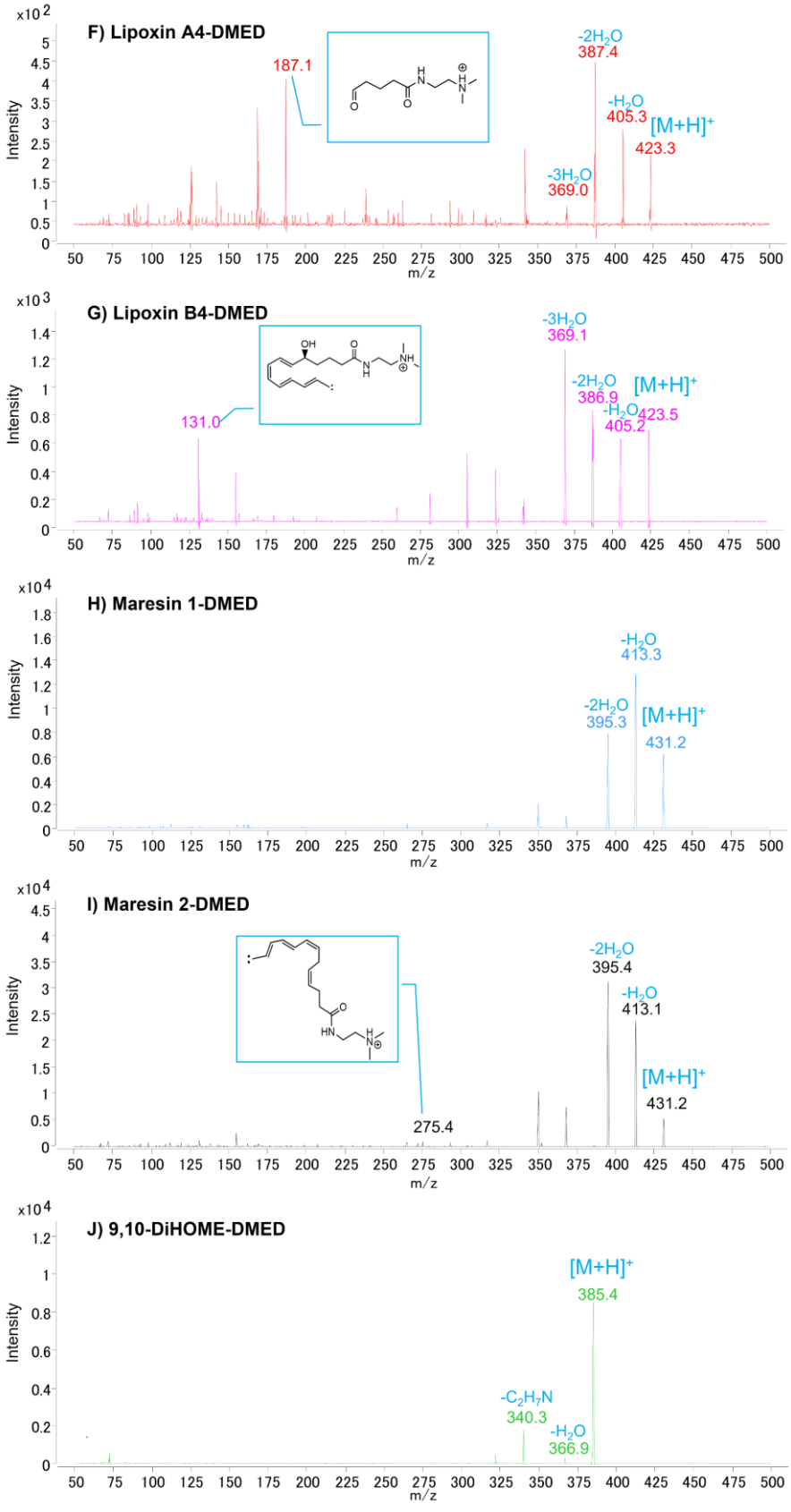
F) Lipoxin A4-DMED
187.1
-2H2O
387.4
-H2O
405.3
[M+H]+
423.3
-3H2O
369.0
G) Lipoxin B4-DMED
-3H2O
369.1
-2H2O
386.9
[M+H]+
-H2O
405.2
423.5
131.0
H) Maresin 1-DMED
-H2O
413.3
-2H2O
395.3
[M+H]+
431.2
I) Maresin 2-DMED
-2H2O
395.4
-H2O
413.1
[M+H]+
431.2
275.4
J) 9,10-DiHOME-DMED
[M+H]+
385.4
-C2H7N
340.3
-H2O
366.9
Intensity
m/z

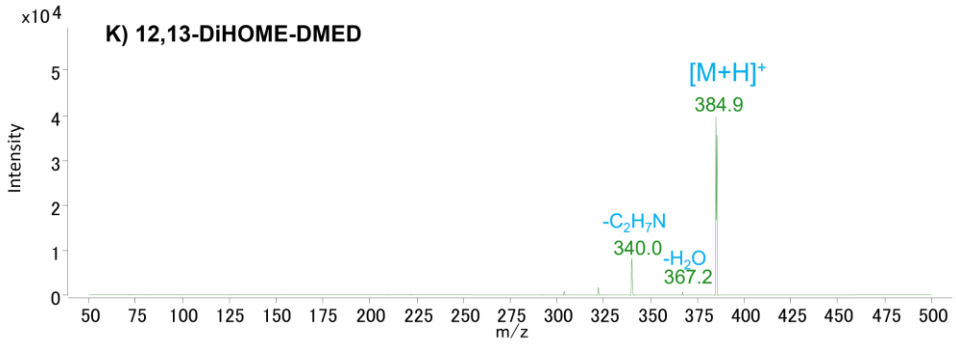

Figure 9. Product ion spectra of eleven different PUFAs derivatized with DMED. PUFAs with allylic vicinal diols (A, B, D–G, I) gave the characteristic fragment ions, whose structures are depicted in the spectra and Figure 8, meanwhile those with the vicinal diols but not at an allylic position, 9,10-DiHOME (J) and 12,13-DiHOME (K), did not. Resolvin D3 (C) and Maresin 1 (H) have the same molecular masses as Resolvin D1, D2, D4, and Maresin 2, respectively (see Table 2.), but not the vicinal diols. 2.5 ng for each were injected into the positive-ion LC/ESI-MS/MS (product ion-scan mode). The retention times for each PUFA were described in Table 2.

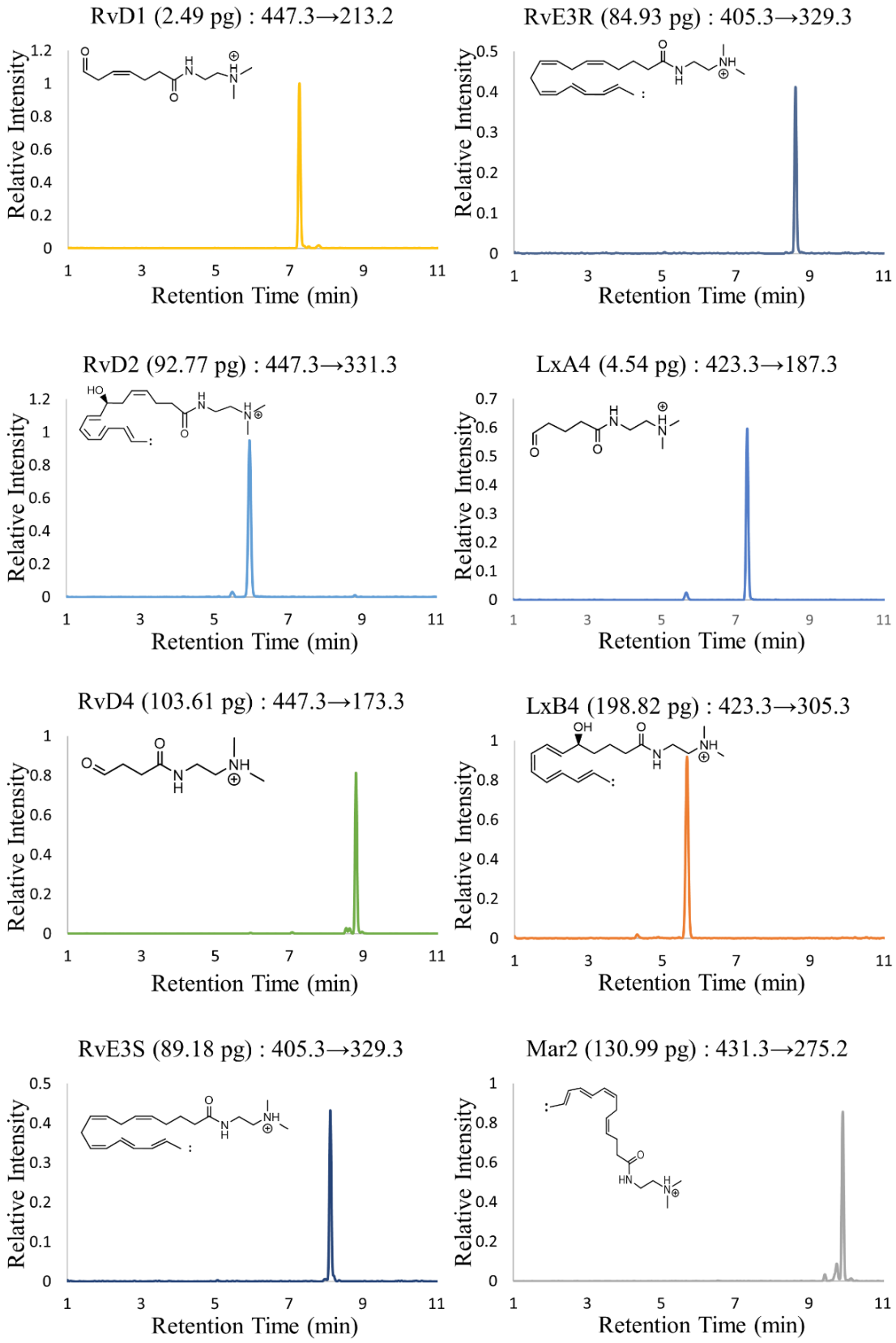

Figure 10. MRM chromatograms of eight kinds of the authentic PUFAs derivatized with DMED. The amounts of each PUFA that were applied to the MRM analysis in LC/ESI-MS/MS were 2.49

pg (RvD1), 92.77 pg (RvD2), 103.61 pg (RvD4), 89.18 pg (RvE3S), 84.93 pg (RvE3R), 4.54 pg (LxA4), 198.82 pg (LxB4), and 130.99 pg (Mar2). Note that the derivatization yield of RvD4 was relatively low despite the fact that an aldehyde type of ion was produced (see Figure 8), which could be attributed to the partial formation of a five-member lactone ring at the carboxyl terminal during derivatization reaction. LxA4, 5S, 6R-Lipoxin A4; LxB4, 5S, 14R-Lipoxin B4; LxA4, 5S, 6R-Lipoxin A4; LxB4, 5S, 14R-Lipoxin B4; Mar2, maresin 2; RvE3S, 18S-Resolvin E3; RvE3R, 18R-Resolvin E3; RvD1, resolvin D1; RvD2, resolvin D2; RvD4, resolvin D4.

II.3-2 Accuracy of the DMED-PUFAs.

The data were processed by quantitative analysis software of the MassHunter Workstation (Agilent) to produce standard curves for each PUFA. The correlation coefficient square (r^2) and accuracies for the seven types of PUFAs based on the characteristic fragment ions were obtained, based on the seven to nine points (M1～M9), and were found to be within acceptable ranges (Figure 11.), which showed good linearity in the ranges of 0.01 - 9.96 nM (RvD1); 0.16 - 20.75 nM (RvD2); 0.26 - 16.60 nM (RvD4); 0.01 - 42.60 nM (LxA4); 0.26 - 33.33 (LxB4); 0.34 - 21.67 nM (Mar2); 0.18 - 23.15 nM (RvE3R), despite the difference in sensitivity. (Table 3.).

(A) RvD1

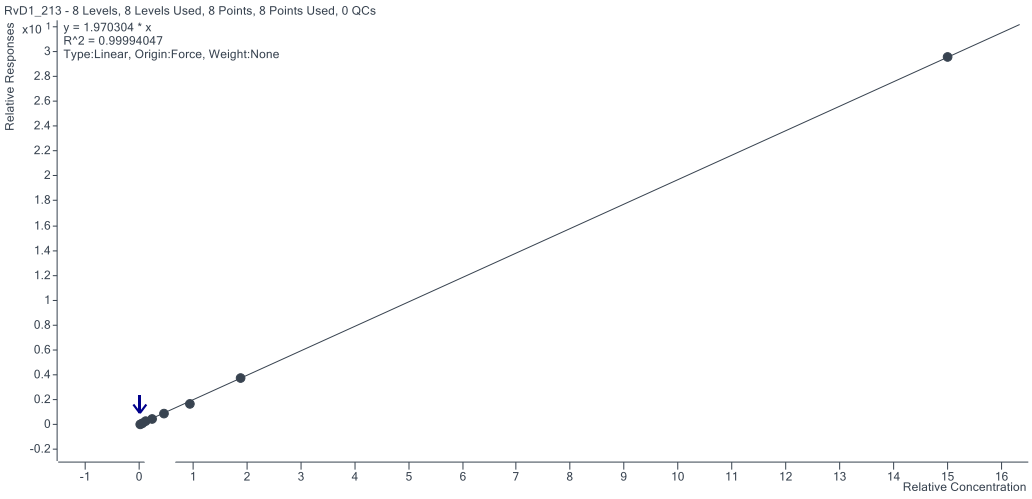

(B) RvD2

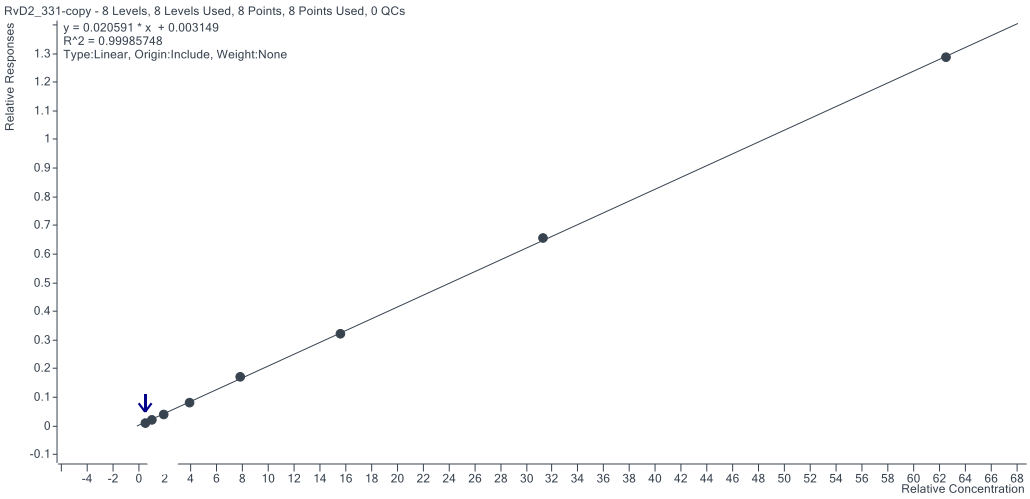

(C) RvD4

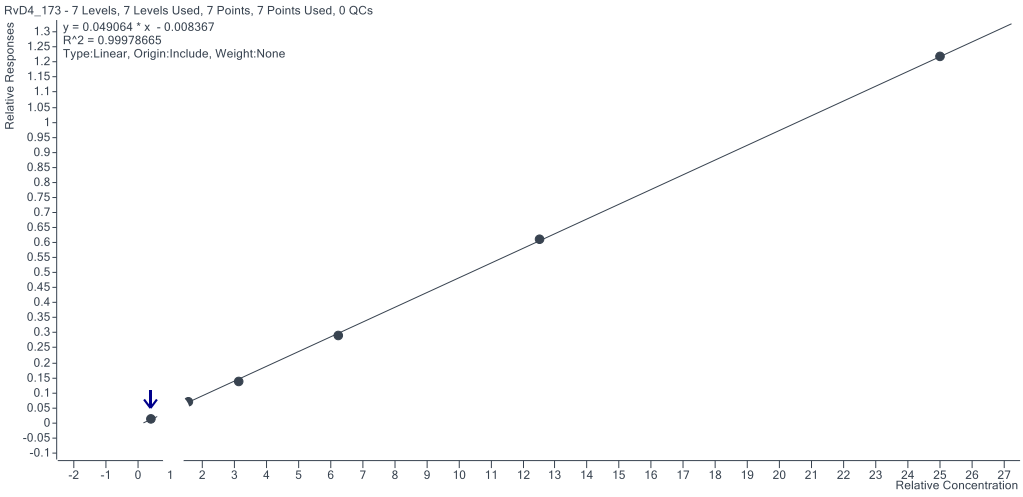

(D) LxA4

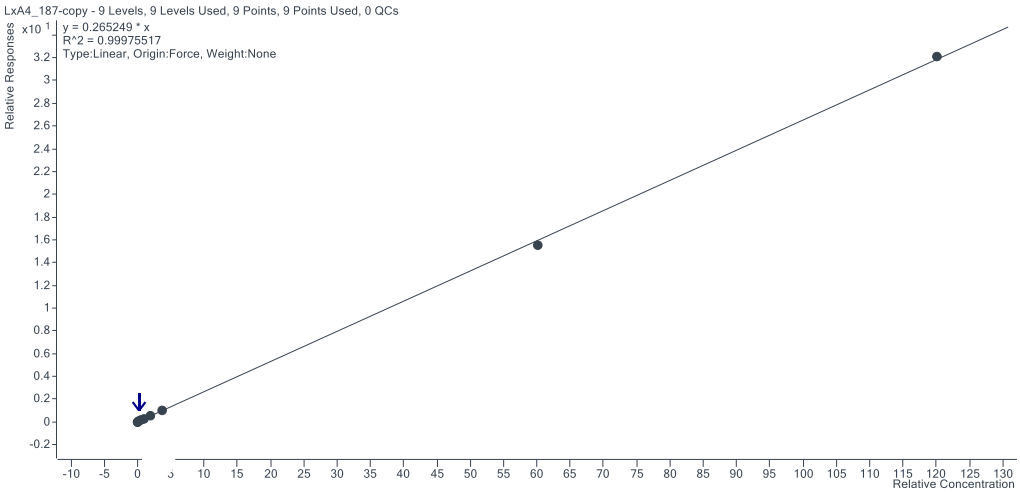

(E) LxB4

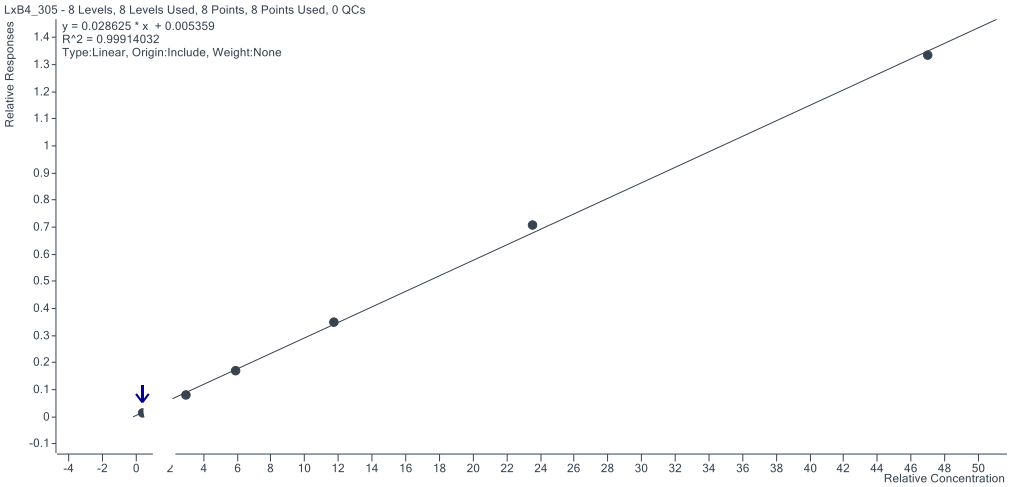

(F) Maresin 2

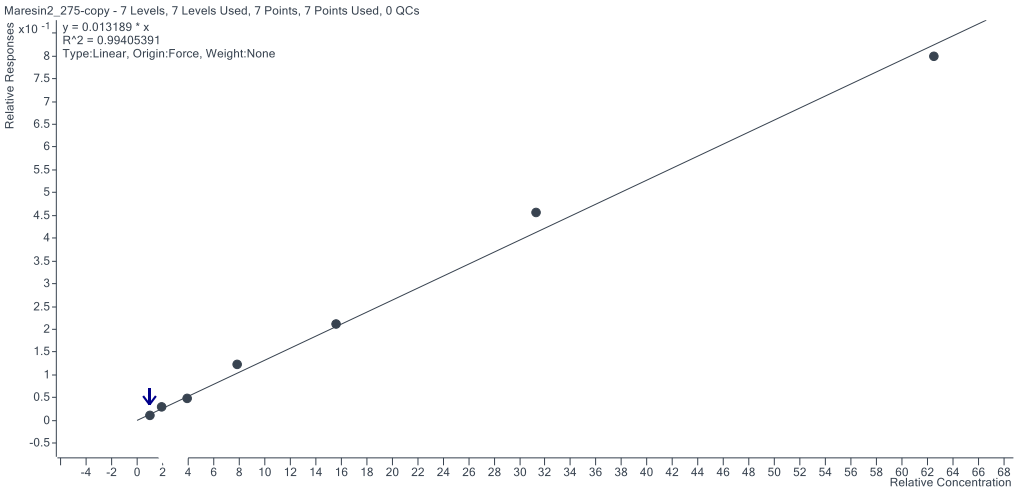

(G) RvE3R

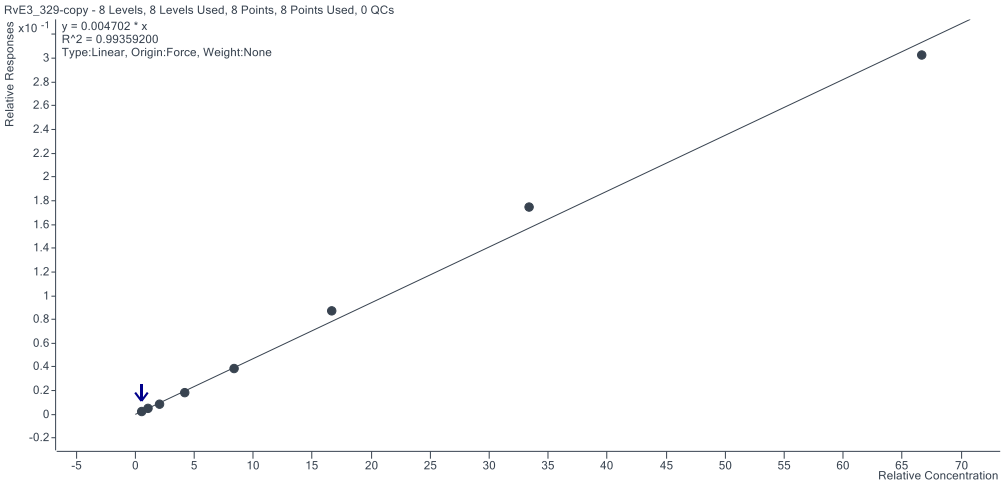

Figure 11. Calibration curves for the LC/ESI-MS/MS analysis of the seven types of PUFAs (see Table 3.).

Table 3. Calibration curves, linearity range, and accuracies of the seven types of PUFAs obtained by this method.

Compound Name & MW	RT (min)	Transition (m/z)	Concentration (nM)	Accuracy	ISTD	Regression Curve		
						k	b	r^2
RvD1 (376.5)	7.13	447.3→213.2	0.01 (M8)	108.0	LxA4-d5	1.9703	0	0.9999
			0.04 (M7)	95.7				
			0.08 (M6)	110.8				
			0.16 (M5)	97.9				
			0.31 (M4)	95.0				
			0.62 (M3)	89.2				
			1.25 (M2)	100.5				
			9.96 (M1)	100.0				
RvD2 (376.5)	5.92	477.3→331.3	0.16 (M8)	88.5	RvD1-d5	0.0206	0.0031	0.9999
			0.32 (M7)	100.4				
			0.65 (M6)	93.7				
			1.30 (M5)	97.6				
			2.59 (M4)	105.4				
			5.19 (M3)	98.6				
			10.38 (M2)	101.4				
			20.75 (M1)	99.7				
RvD4 (376.5)	8.74	447.3→173.3	0.26 (M7)	115.3	LxA4-d5	0.0491	-0.0084	0.9998
			0.52 (M6)	92.9				
			1.04 (M5)	102.3				
			2.08 (M4)	94.8				
			4.15 (M3)	97.1				
			8.30 (M2)	101.0				
			16.60 (M1)	100.0				
LxA4 (352.5)	7.29	423.3→187.3	0.01 (M9)	112.8	RvD1-d5	0.2652	0	0.9998
			0.02 (M8)	106.7				
			0.08 (M7)	87.3				
			0.17 (M6)	105.1				
			0.33 (M5)	101.2				
			0.67 (M4)	100.4				
			1.33 (M3)	98.6				
			21.30 (M2)	97.2				
			42.60 (M1)	100.7				

LxB4 (352.5)	5.67	423.3→305.3	0.26 (M8)	94.2	LxA4-d5	0.0287	0.006	0.9991
			0.52 (M7)	109.5				
			1.04 (M6)	85.7				
			2.08 (M5)	88.6				
			4.17 (M4)	98.7				
			8.33 (M3)	102.5				
			16.66 (M2)	104.4				
			33.33 (M1)	98.8				
Maresin2 (360.5)	9.83	431.3→275.2	0.34 (M7)	89.6	RvD1-d5	0.0132	0	0.9941
			0.68 (M6)	115.9				
			1.35 (M5)	95.5				
			2.71 (M4)	118.5				
			5.42 (M3)	102.9				
			10.84 (M2)	110.6				
			21.67 (M1)	96.9				
RvE3R (360.0)	8.69	405.3→329.3	0.18 (M8)	101.3	RvD1-d5	0.0098	0	0.9936
			0.36 (M7)	111.0				
			0.72 (M6)	85.5				
			1.45 (M5)	93.6				
			2.89 (M4)	99.4				
			5.79 (M3)	111.0				
			11.57 (M2)	111.4				
			23.15 (M1)	96.5				

II.3-3 Comparison of sensitivity between DMED-derivatized and free PUFAs

By using the PUFA standards, negative-ion mode method, described previously (40), and positive-ion mode obtained above were compared. The correlation coefficient square (r^2) and accuracies for the 6 types of PUFAs, based on the transitions described previously, were obtained (Table. 4b). In comparison with the results of the positive-ion mode (Table. 4a), negative-ion mode has lower sensitivity and accuracy, except for Maresin 2. Thus, the measurement of these PUFAs derivatized with the cationic compound is apparently advantageous over the measurement of free ones in negative-ion mode.

Table 4. Comparison of the sensitivity of PUFAs derivatized with DMED (positive-ion mode) with free ones (negative-ion mode).

a. Positive-ion mode (DMED-PUFA). This table is re-edited from Table 3.

Compound Name	RT (min)	Transition (m/z)	Linearity range (nM)	r^2	Accuracy range	ISTD
RvD1	7.1	447.3→213.2	0.01 - 9.96	0.9999	89.2 - 110.8	LxA4-d5
RvD2	5.9	477.3→331.3	0.16 - 20.75	0.9999	88.5 - 105.4	RvD1-d5
RvD4	8.7	447.3→173.3	0.26 - 16.60	0.9998	92.9 - 115.3	LxA4-d5
LxA4	7.3	423.3→187.3	0.01 - 42.60	0.9998	87.3 - 112.8	RvD1-d5
LxB4	5.7	423.3→305.3	0.26 – 33.33	0.9991	85.7 – 109.5	LxA4-d5
Maresin2	9.8	431.3→275.2	0.34 – 21.67	0.9941	89.6 - 118.5	RvD1-d5
RvE3R	8.6	405.3→329.3	0.18 – 23.15	0.9936	85.5 – 111.4	RvD1-d5

b. Negative-ion mode (Free PUFA)

Compound Name	RT (min)	Transition* (m/z)	Linearity range (nM)	r^2	Accuracy range	ISTD
RvD1_135	4.5	375.0→135.0	0.52 - 66.40	0.9990	80.8 - 135.7	RvD1-d5
RvD1_233	4.5	375.0→233.0	0.52 - 66.40	0.9991	97.6 - 240.3	LxA4-d5
RvD2	4.1	375.0→203.0	2.59 – 332.01	0.9940	89.1 - 390.9	LxA4-d5
RvD4	5.3	375.0→131.0	0.69 - 88.53	0.9998	89.4 - 129.0	LxA4-d5
LxA4	4.5	351.0→217.0	0.92 - 118.20	0.9997	96.1 - 156.2	LxA4-d5
LxB4	3.9	351.0→221.0	0.69 – 88.65	0.9979	86.5 - 116.5	RvD1-d5
Maresin2_177	7.4	359.0→177.0	0.34 – 43.34	0.9999	49.0 - 108.0	RvD1-d5
Maresin2_221	7.4	359.0→221.0	0.34 - 43.34	0.9999	92.2 - 109.5	LxA4-d5

*The transitions were those described in R.A. Colas, *et al.* Am. J. Physiol. Cell Physiol. 2014.

The accuracies of standard curves beyond the acceptable range (85-115%) are shown in red, those at the lower limit of quantification can be within 80-120%.

Chapter III. Analysis of PUFAs that have Allylic Vicinal Diols in Human Serum

III.1 Introduction

As described in "General Introduction 1.2", the PUFAs that have allylic vicinal diols, which are dealt with in this thesis, are especially classified in "specialized pro-resolving mediators" that have a powerful biological activity when given in the body. Therefore, there have been many reports on their detection using human body fluids or tissues, and their biological and clinical relevance have been discussed (5, 7).

In this chapter, the diagnostic ions of eight kinds of PUFAs that have been characterized and established in Chapter II (Table 2, Figure 10.) have been applied for screening those PUFAs in human serum samples, which were commercially obtained from healthy volunteers (20-36 ages).

III.2 Materials and Methods

III.2-1 Chemicals

Chemicals are the same as in Chapter II.

III.2-2 Human sera and ethical approval.

Samples of human sera (584-male (23 y.o.), 585-male (20 y.o.), 587-male (36 y.o.), 588-male (32 y.o.), 589-male (36 y.o.), 590-male (34 y.o.), 591-male (32 y.o.), 593-female (28 y.o.), 594-female (25 y.o.), 597-female (34 y.o.), and 600-female (30 y.o.)) without personally identifiable information were purchased from BioIVT (Hicksville, NY). This study was approved by the Ethics Committee of the Institute for Protein Research, Osaka University (No. 2021-1-1). Human studies abided by the Declaration of Helsinki principles.

III.2-3 Preparation of DMED-derivatized serum PUFAs

The PUFAs were isolated from serum according to a previously reported method with minor modifications (41, 42). 20 µL of aliquots from eight healthy volunteers ages 20-36 (see above) were spiked with LxA4d (17.48 pg) and RvD1d (8.19 pg) as the internal standards. The pre-spiked sample was mixed with 100 µL of a 90% ACN/10% MeOH solution containing 0.01mM BHT, vortexed, allowed to stand at

room temperature for 30 min and then centrifuged for 15 min at 12,000 rpm. The supernatant was diluted eight times with ultrapure water, and then loaded on a Bond Elute C18 column (50 mg) that had been washed with 1 mL of aqueous 70% ACN/0.3% FA and equilibrated with 2 mL of aqueous 5% ACN/0.3% FA. After washing the column twice with 1 mL of 5% ACN/0.3% FA, the PUFAs were eluted with 800 μL of aqueous 45% ACN/0.3% FA. The eluates were evaporated to dryness, derivatized with DMED as above, and subjected to LC-MS/MS for the MRM analysis (see below).

III.2-4 LC-MS/MS.

The LC-MS/MS method is the same as in Chapter II.

III.2-5 Recoveries and Precisions.

The recoveries of the six types of PUFAs, except for RvE3, from serum were assessed as follows: Two concentrations (x1 and x4), which were set for each standard PUFA on the basis of the detection responses of each transition (see Figure 10), were examined in ten separate experiments. Each of the x1 and x4 concentrations of a mixture of the six kinds of PUFAs, dissolved in 12 μL of DMF, was added to 20 μL of "590-female" serum and treated as described above. The resulting eluate was dried under a vacuum, derivatized with DMED in the same manner as described above, and finally, spiked with IS that had been derivatized with DMED ("pre-spike"). In parallel, the same serum as that above, but without spiking, was treated similar to the above sample. Each resulting eluate was spiked with ×1 and ×4 concentrations of a mixture of PUFAs, dried, derivatized, and then, spiked with DMED-derivatized IS ("post-spike"). The recoveries of each PUFA were calculated as $H_{pre\text{-}spike}/H_{post\text{-}spike}$ x 100, where H is the peak height of the compound in MRM, which had been normalized by the peak heights of LxA4-d5 or RvD1-d5 in IS, and represented the average of ten separate experiments. The recoveries of each compound for the present procedure including the DMED derivatization ranged from 61.9 to 74.9% (Table. 5). In addition, the precision of the method was assessed by RSDs (relative standard deviation), which were calculated, based on the peak heights of each compound obtained for ten separate preparations of post-spike sera samples (Table. 5).

III.3 Results and Discussion

III.3-1 Recoveries and precisions of the measurement of the PUFAs in human serum

The recoveries of the PUFAs from human serum were estimated to range from 61.9 to 74.9% (n = 10) (Table. 5), based on the peak height ratios of the six types of PUFAs in a “pre-spike” sample to those in a “post-spike” sample (see III.2-5). In addition, the precision (stability) of the present method was assessed by measuring two different concentrations of standard mixtures. The relative standard deviations (RSD) were calculated for the peak heights of the six types of PUFAs in the post-spike samples obtained for ten separate preparations. The RSDs for each PUFA were within acceptable ranges (4.10 to 12.97% in Table. 5).

Table 5. Recovery and precision of the method. Human serum was spiked with a mixture of RvD1, RvD2, RvD4, LxA4, LxB4, and Mar2. Two concentrations (x1 and x4) of each standard, which were set on the basis of the detection responses of each transition, were examined in ten separate experiments.

Compound Name	Spiked Concentration (nM)	Recovery (%) n=10		Precision (%) n=10
		Mean (%)	RSD (%)	
RvD1	1.95	70.03	7.89	7.61
	0.49	65.67	10.68	10.38
RvD2	48.63	71.01	6.98	7.82
	12.16	65.93	9.19	7.63
RvD4	149.64	64.65	10.47	9.48
	37.41	65.30	9.08	6.32
LxA4	7.56	67.56	14.46	8.85
	1.89	74.91	12.18	12.97
LxB4	79.92	68.26	7.37	7.88
	19.98	68.51	10.98	4.10
Maresin2	123.89	69.89	12.55	9.42
	30.97	61.90	15.61	5.27

III.3-2 Detection and quantitative analysis of PUFAs in human serum

The MRM analysis, based on the diagnostic ions that are characteristic for allylic vicinal diol-containing PUFAs, allowed RvD1, RvD2, RvE3S, RvE3R, LxA4, and LxB4 among the eight types of the PUFAs to be detected in human serum (Table. 6). They were distinctly observed at the same retention times as those for the authentic PUFAs and those spiked in serum (Figure 12) although several unknown peaks were still observed for each MRM transition. Meanwhile, the MRM chromatograms for their doubly dehydrated fragment ions (447.3 -> 411.3 for RvD1, RvD2 and RvD4; 423.3 -> 387.4 for LxA4 and LxB4), which are typically used as the MRM transitions and are the most intense ion peaks in the positive-ion MS/MS (see Figure 9.), showed a considerable number of peaks (Figure 13), which makes quantification of those PUFAs quite difficult. The other PUFAs (RvD4 and Mar2) were hardly detected or indistinguishable from ghost peaks in sera used in this study (Table 6).

The abundances of the six types of PUFAs observed in commercially obtained human sera, varied from individual to individual, among which the samples from “585-male” and “587-male” contained much lower levels of these PUFAs. Moreover, RvD1, LxA4, and LxB4 were observed in all of the samples, and LxA4 and LxB4 were the predominant PUFAs that were detected, the amounts of which were apparently correlated with each other (Table 6). It is noteworthy in this respect that these PUFAs are classified as the anti-inflammatory and pro-resolving lipid mediators and therefore have the potential to serve as a biomarker for diseases such as asthma (5) despite the fact that the physiological states derived from those sera were not disclosed.

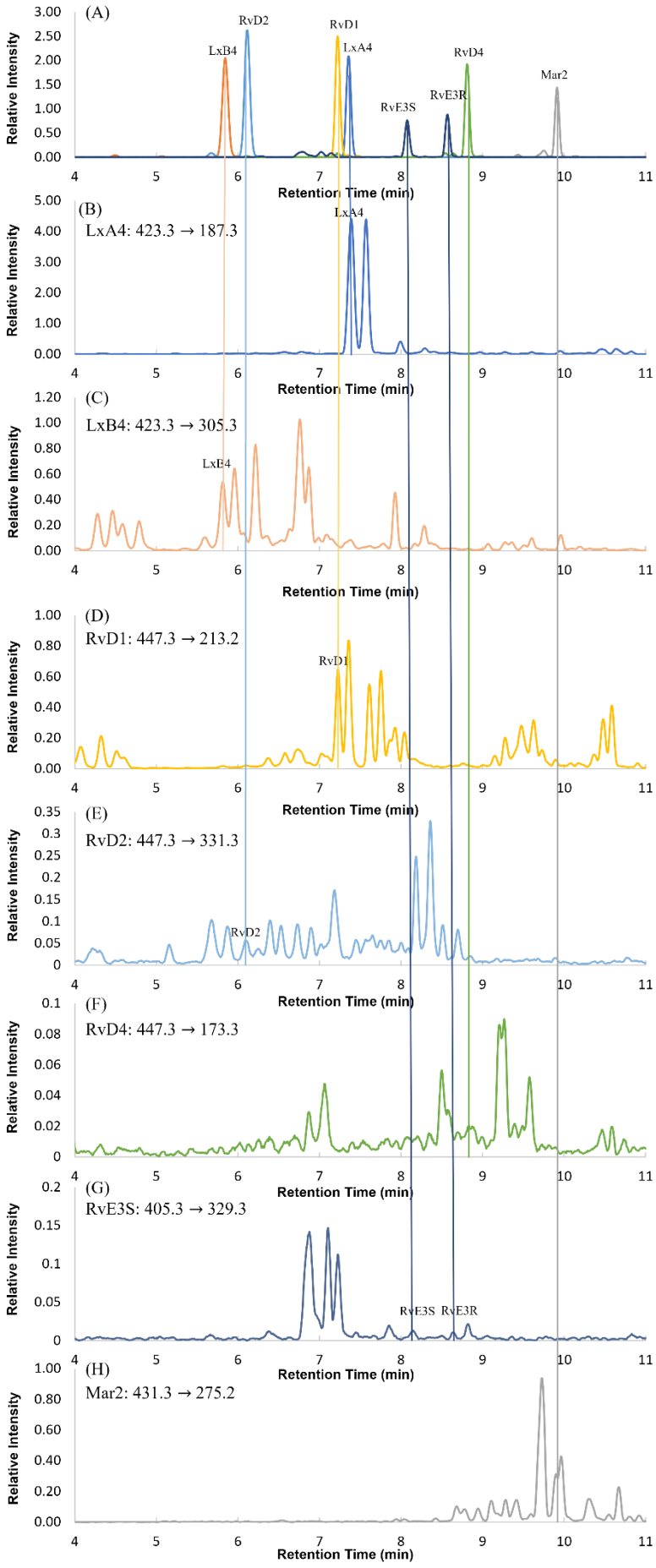
(A)
LxB4
RvD2
RvD1
LxA4
RvE3S
RvE3R
RvD4
Mar2
(B)
LxA4: 423.3 → 187.3
(C)
LxB4: 423.3 → 305.3
(D)
RvD1: 447.3 → 213.2
(E)
RvD2: 447.3 → 331.3
(F)
RvD4: 447.3 → 173.3
(G)
RvE3S: 405.3 → 329.3
(H)
Mar2: 431.3 → 275.2
Relative Intensity
Retention Time (min)

Figure 12. MRM chromatograms of eight types of authentic PUFAs derivatized with DMED (A) and actual samples derived from human serum ("594-female") treated and derivatized with DMED as described in **III.2-3** (B-H). The MRM chromatograms were extracted from a single measurement, based on the characteristic MRM transitions for each PUFA (Table 2.). The authentic PUFAs in (A) were the same as those in Figure 10.

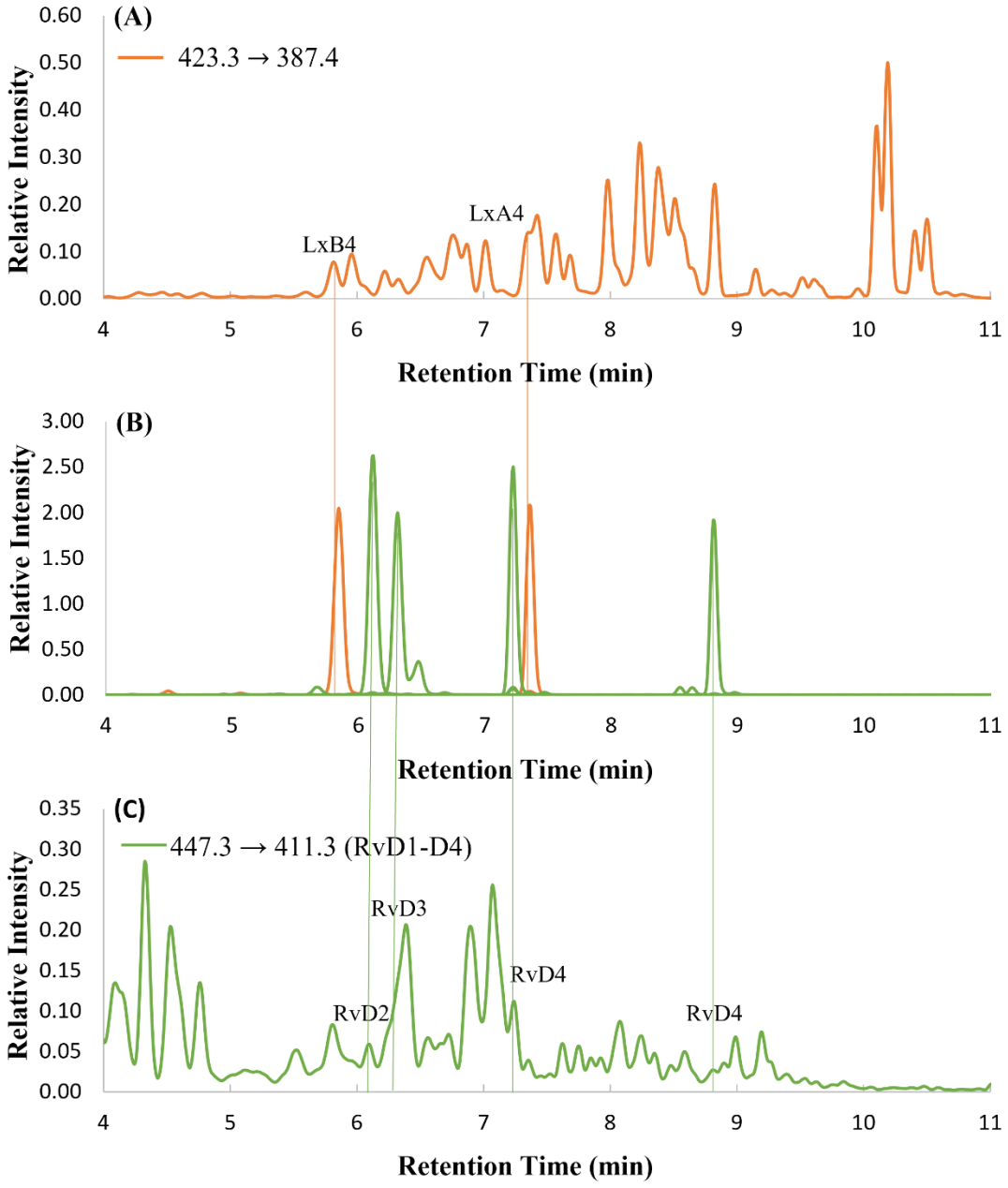

Figure 13. MRM chromatograms of the doubly dehydrated fragment ions derived from isobaric LxA4 and LxB4 (A) and from isobaric RvD1-D4 (C), and those observed for the standard mixture (B), which were reconstituted from the data shown in Figure 12.

Table 6. Summary of the quantitation of the PUFAs in eight specimens of human sera (see Figure 12.).

Sample Name	Concentration (nM) n=3							
	RvD1 (LxA4-d5)	RvD2 (RvD1-d5)	RvD4 (LxA4-d5)	LxA4 (RvD1-d5)	LxB4 (LxA4-d5)	Maresin2 (RvD1-d5)	RvE3S (RvD1-d5)	RvE3R (RvD1-d5)
584M	1.76 ±0.03	3.61 ±0.11	N.D.	55.30 ±1.82	76.29 ±3.53	N.D.	1.46 ±0.60	1.55 ±0.81
588M	0.23 ±0.01	0	N.D.	7.27 ±0.09	10.14 ±0.10	N.D.	0	0
589M	1.41 ±0.90	0	N.D.	8.79 ±0.11	17.52 ±0.54	N.D.	3.39 ±0.11	2.42 ±0.28
591M	0.19 ±0.01	0	N.D.	2.50 ±0.09	3.58 ±0.35	N.D.	0	0
593F	1.82 ±0.08	3.56 ±0.06	N.D.	39.35 ±0.96	52.14 ±1.65	N.D.	3.03 ±0.09	0.93 ±0.12
594F	3.02 ±0.18	7.18 ±0.24	N.D.	52.52 ±1.63	88.32 ±3.18	N.D.	3.22 ±0.12	1.77 ±0.32
597F	1.90 ±0.12	3.99 ±0.18	N.D.	7.73 ±0.12	25.01 ±1.21	N.D.	14.46 ±0.74	9.49 ±0.59
600F	0.15 ±0.01	0	N.D.	3.15 ±0.03	4.17 ±0.31	N.D.	0	0

III.3-3 Analysis of free PUFAs in human serum

The issue of whether or not the present PUFAs could be detected in serum using the negative-ion mode according to the method described previously (40) was evaluated. However, starting from a 20 µL volume of serum (the same amount as used in the above), it was not possible to identify the PUFAs using the current sample size and pretreatment protocol used in this study (Figure 14.). This can be attributed to, not only the lower sensitivity in the negative-ion mode, but also a heavy matrix effect derived from the serum itself.

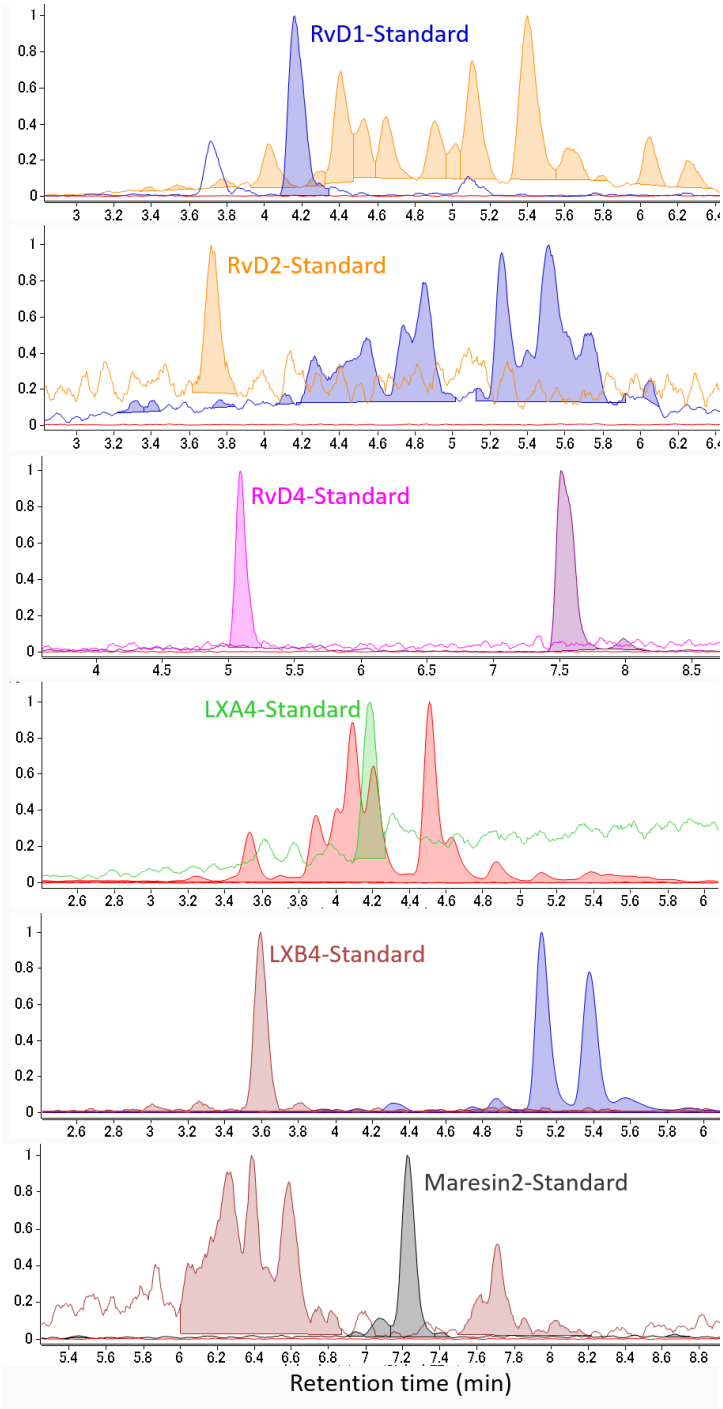

Figure 14. MRM chromatograms of the PUFAs in 20 µL serum sample and free PUFA standards.

General Conclusion

Since the PUFAs could be structurally classified by the number of carbons, hydroxyl groups, and carbon-carbon double bonds that they contain, and each has the same molecular mass, there are many structural isomers that are defined by the difference in the position of the double bonds and hydroxyl group(s), and in their configurations. Thus, in order to clearly identify and quantify these molecules by MRM analysis, especially those in a complex mixture, it is necessary to use characteristic fragment ions that are specific for each of them (43), as the diagnostic ions. Negative-ion MS/MS is advantageous for this type of analysis since it produces various skeleton-derived fragment ions, it is not always the choice of measurement for the analysis of PUFAs in a limited amount of bio-sample because of the low sensitivity associated with this method. On the other hand, chemical derivatization with cationic compounds such as DMED (35) or AMPP (36, 37) significantly elevate the sensitivity of this type of analysis by from hundred and ten to twenty times higher, respectively, in the positive-ion mode ESI-MS/MS compared to the negative-ion mode. These derivatized fatty acids showed charge-remote fragmentation, which, in general, could result in a simple fragmentation containing a cationic tag. In the case of the AMPP tag (not commercially available), intense fragment ions derived from the cationic tag portions were observed in the low m/z region when a relatively high CE voltage was used, the conditions of which also allowed ions derived from fatty acid chains to be detected, which could be useful for their characterization. Meanwhile, DMED, a versatile derivatizing reagent, predominantly retains a proton in the positive-ion mode. This proton as well as those at hydroxyl group protons could be mobile in the molecule during CID, thereby, significantly promoting dehydration, which was also involved with the current fragmentation at vicinal diols (Scheme 3). This, however, has not been observed for an AMPP-derivatized fatty acid since it has a fixed charge site and does not contain any mobile protons. The higher sensitivity obtained in the case of the DMED derivatization is, thus, attributed to high abundance of ions derived from multiple dehydration processes (see Figure 9). However, since the same MRM transitions, pairs of molecular masses and those of the dehydrated or degraded ions, are applied for the isobaric isomers, they cannot be differentiated by the MRM transitions and, as a result, they are only distinguishable by the retention times in LC. This issue becomes more problematic when being applied to a complex mixture such as a bio-sample which contains various contaminants that generate numerous unknown peaks over the analysis range since they are occasionally

observed to have the same transitions as target compounds (see Figure 13).

The characteristic fragmentation occurring at the allylic vicinal diols, which is derived from a dehydration process promoted by a mobile proton (Scheme 3), is useful for characterizing RvD1, RvD2, and RvD4; LxA4 and LxB4; Mar2, and RvE3 in the positive-ion ESI-MS/MS. LxA4, LxB4, RvD1, RvD2, and RvE3, which are bioactive autacoids with anti-inflammatory or pro-resolving capabilities (5, 44), could be observed for healthy volunteers' sera (20-36 ages), which were commercially obtained. In addition, since the present analysis was demonstrated to be feasible for use with a 20 μL aliquot of serum, this made sample pretreatment easy and could be applied to limited amounts of clinical samples or those obtained from living bodies.

List of Publication

Huibin Zhu, Mone Kurokawa, Mengyao Chen, Qiuyi Wang, Masayuki Inoue, and Toshifumi Takao (2023) Characteristic fragmentation of polyunsaturated fatty acids with allylic vicinal diols in positive-ion LC/ESI-MS/MS. ***J. Lipid Research***, 64(6) 100384.

References

1. Watanabe, Y., and I. Tatsuno. 2020. Prevention of cardiovascular events with omega-3 polyunsaturated fatty acids and the mechanism involved. *Journal of atherosclerosis and thrombosis* **27**: 183-198.
2. Hansen, T. V., and C. N. Serhan. 2022. Protectins: Their biosynthesis, metabolism and structure-functions. *Biochemical Pharmacology*: 115330.
3. Fierro, I., and C. Serhan. 2001. Mechanisms in anti-inflammation and resolution: the role of lipoxins and aspirin-triggered lipoxins. *Brazilian Journal of Medical and Biological Research* **34**: 555-566.
4. Tapiero, H., G. N. Ba, P. Couvreur, and K. Tew. 2002. Polyunsaturated fatty acids (PUFA) and eicosanoids in human health and pathologies. *Biomedicine & pharmacotherapy* **56**: 215-222.
5. Serhan, C. N., and B. D. Levy. 2018. Resolvins in inflammation: emergence of the pro-resolving superfamily of mediators. *The Journal of clinical investigation* **128**: 2657-2669.
6. Bento, A. F., R. F. Claudino, R. C. Dutra, R. Marcon, and J. B. Calixto. 2011. Omega-3 Fatty Acid-Derived Mediators 17(R)-Hydroxy Docosahexaenoic Acid, Aspirin-Triggered Resolvin D1 and Resolvin D2 Prevent Experimental Colitis in Mice. *The Journal of Immunology* **187**: 1957-1969.
7. Serhan, C. N. 2014. Pro-resolving lipid mediators are leads for resolution physiology. *Nature* **510**: 92-101.
8. Serhan, C. N., J. Dalli, R. A. Colas, J. W. Winkler, and N. Chiang. 2015. Protectins and maresins: New pro-resolving families of mediators in acute inflammation and resolution bioactive metabolome. *Biochimica et Biophysica Acta (BBA)-Molecular and Cell Biology of Lipids* **1851**: 397-413.
9. Gu, Z., G. J. Lamont, R. J. Lamont, S. M. Uriarte, H. Wang, and D. A. Scott. 2016. Resolvin D1, resolvin D2 and maresin 1 activate the GSK3β anti-inflammatory axis in TLR4-engaged human monocytes. *Innate immunity* **22**: 186-195.
10. Lannan, K. L., S. L. Spinelli, N. Blumberg, and R. P. Phipps. 2017. Maresin 1 induces a novel pro-resolving phenotype in human platelets. *Journal of Thrombosis and Haemostasis*

15: 802-813.
11. Ledard, N., A. Liboz, B. Blondeau, M. Babiak, C. Moulin, B. Vallin, I. Guillas, V. Mateo, C. Jumeau, and K. Blirando. 2020. Slug, a cancer-related transcription factor, is involved in vascular smooth muscle cell transdifferentiation induced by platelet-derived growth factor-BB during atherosclerosis. *Journal of the American Heart Association* **9**: e014276.
12. Panigrahy, D., M. M. Gilligan, C. N. Serhan, and K. Kashfi. 2021. Resolution of inflammation: An organizing principle in biology and medicine. *Pharmacology & therapeutics* **227**: 107879.
13. Kain, V., K. A. Ingle, R. A. Colas, J. Dalli, S. D. Prabhu, C. N. Serhan, M. Joshi, and G. V. Halade. 2015. Resolvin D1 activates the inflammation resolving response at splenic and ventricular site following myocardial infarction leading to improved ventricular function. *Journal of molecular and cellular cardiology* **84**: 24-35.
14. Chiurchiù, V., A. Leuti, J. Dalli, A. Jacobsson, L. Battistini, M. Maccarrone, and C. N. Serhan. 2016. Proresolving lipid mediators resolvin D1, resolvin D2, and maresin 1 are critical in modulating T cell responses. *Science translational medicine* **8**: 353ra111-353ra111.
15. Minihane, A. M., and J. Lovegrove. 2006. Health benefits of polyunsaturated fatty acids (PUFAs). *In* Improving the fat content of foods. Elsevier. 107-140.
16. Seppänen-Laakso, T., I. Laakso, and R. Hiltunen. 2002. Analysis of fatty acids by gas chromatography, and its relevance to research on health and nutrition. *Analytica Chimica Acta* **465**: 39-62.
17. Brondz, I. 2002. Development of fatty acid analysis by high-performance liquid chromatography, gas chromatography, and related techniques. *Analytica Chimica Acta* **465**: 1-37.
18. Chen, S.-H., and Y.-J. Chuang. 2002. Analysis of fatty acids by column liquid chromatography. *Analytica Chimica Acta* **465**: 145-155.
19. Li, G., J. You, Y. Suo, C. Song, Z. Sun, L. Xia, X. Zhao, and J. Shi. 2011. A developed pre-column derivatization method for the determination of free fatty acids in edible oils by reversed-phase HPLC with fluorescence detection and its application to Lycium barbarum seed oil. *Food Chemistry* **125**: 1365-1372.
20. Fahy, E., S. Subramaniam, H. A. Brown, C. K. Glass, A. H. Merrill, R. C. Murphy, C. R. Raetz, D. W. Russell, Y. Seyama, and W. Shaw. 2005. A comprehensive classification system for lipids1. *Journal of lipid research* **46**: 839-861.
21. Liebisch, G., E. Fahy, J. Aoki, E. A. Dennis, T. Durand, C. S. Ejsing, M. Fedorova, I. Feussner, W. J. Griffiths, and H. Köfeler. 2020. Update on LIPID MAPS classification, nomenclature, and shorthand notation for MS-derived lipid structures. *Journal of lipid research* **61**: 1539-1555.
22. Xu, F., L. Zou, Y. Liu, Z. Zhang, and C. N. Ong. 2011. Enhancement of the capabilities

of liquid chromatography–mass spectrometry with derivatization: general principles and applications. *Mass spectrometry reviews* **30**: 1143-1172.
23. Higashi, T., and S. Ogawa. 2016. Isotope-coded ESI-enhancing derivatization reagents for differential analysis, quantification and profiling of metabolites in biological samples by LC/MS: A review. *Journal of pharmaceutical and biomedical analysis* **130**: 181-193.
24. Zhu, Q.-F., Z. Zhang, P. Liu, S.-J. Zheng, K. Peng, Q.-Y. Deng, F. Zheng, B.-F. Yuan, and Y.-Q. Feng. 2016. Analysis of liposoluble carboxylic acids metabolome in human serum by stable isotope labeling coupled with liquid chromatography–mass spectrometry. *Journal of Chromatography A* **1460**: 100-109.
25. Xiong, C.-F., Q.-F. Zhu, Y.-Y. Chen, D.-X. He, and Y.-Q. Feng. 2021. Screening and identification of epoxy/dihydroxy-oxylipins by chemical labeling-assisted ultrahigh-performance liquid chromatography coupled with high-resolution mass spectrometry. *Analytical Chemistry* **93**: 9904-9911.
26. Thomas, D., M. Morris, J. M. Curtis, and R. K. Boyd. 1995. Fragmentation mechanisms of protonated actinomycins and their use in structural determination of unknown analogues. *Journal of Mass Spectrometry* **30**: 1111-1125.
27. Skolnik, J. M., J. S. Barrett, H. Shi, and P. C. Adamson. 2006. A liquid chromatography-tandem mass spectrometry method for the simultaneous quantification of actinomycin-D and vincristine in children with cancer. *Cancer chemotherapy and pharmacology* **57**: 458-464.
28. Wheelan, P., J. A. Zirrolli, and R. C. Murphy. 1996. Electrospray ionization and low energy tandem mass spectrometry of polyhydroxy unsaturated fatty acids. *J Am Soc Mass Spectrom* **7**: 140-149.
29. Kerwin, J. L., A. M. Wiens, and L. H. Ericsson. 1996. Identification of fatty acids by electrospray mass spectrometry and tandem mass spectrometry. *Journal of mass spectrometry* **31**: 184-192.
30. Griffiths, W. J., Y. Yang, J. Sjövall, and J. Å. Lindgren. 1996. Electrospray/collision-induced dissociation mass spectrometry of mono-, di-and tri-hydroxylated lipoxygenase products, including leukotrienes of the B-series and lipoxins. *Rapid communications in mass spectrometry* **10**: 183-196.
31. Le Faouder, P., V. Baillif, I. Spreadbury, J.-P. Motta, P. Rousset, G. Chêne, C. Guigné, F. Tercé, S. Vanner, and N. Vergnolle. 2013. LC–MS/MS method for rapid and concomitant quantification of pro-inflammatory and pro-resolving polyunsaturated fatty acid metabolites. *Journal of Chromatography B* **932**: 123-133.
32. Hong, S., Y. Lu, R. Yang, K. H. Gotlinger, N. A. Petasis, and C. N. Serhan. 2007. Resolvin D1, protectin D1, and related docosahexaenoic acid-derived products: analysis via electrospray/low energy tandem mass spectrometry based on spectra and fragmentation mechanisms. *Journal of the American Society for Mass Spectrometry* **18**: 128-144.

33. Hu, T., C. Tie, Z. Wang, and J. L. Zhang. 2017. Highly sensitive and specific derivatization strategy to profile and quantitate eicosanoids by UPLC-MS/MS. *Anal Chim Acta* **950**: 108-118.
34. Matuszewski, B. K., M. Constanzer, and C. Chavez-Eng. 2003. Strategies for the assessment of matrix effect in quantitative bioanalytical methods based on HPLC− MS/MS. *Analytical chemistry* **75**: 3019-3030.
35. Zhu, Q. F., Y. H. Hao, M. Z. Liu, J. Yue, J. Ni, B. F. Yuan, and Y. Q. Feng. 2015. Analysis of cytochrome P450 metabolites of arachidonic acid by stable isotope probe labeling coupled with ultra high-performance liquid chromatography/mass spectrometry. *J Chromatogr A* **1410**: 154-163.
36. Bollinger, J. G., W. Thompson, Y. Lai, R. C. Oslund, T. S. Hallstrand, M. Sadilek, F. Turecek, and M. H. Gelb. 2010. Improved sensitivity mass spectrometric detection of eicosanoids by charge reversal derivatization. *Analytical chemistry* **82**: 6790-6796.
37. Wang, M., R. H. Han, and X. Han. 2013. Fatty acidomics: global analysis of lipid species containing a carboxyl group with a charge-remote fragmentation-assisted approach. *Analytical chemistry* **85**: 9312-9320.
38. Urabe, D., H. Todoroki, K. Masuda, and M. Inoue. 2012. Total syntheses of four possible stereoisomers of resolvin E3. *Tetrahedron* **68**: 3210-3219.
39. Isobe, Y., M. Arita, R. Iwamoto, D. Urabe, H. Todoroki, K. Masuda, M. Inoue, and H. Arai. 2013. Stereochemical assignment and anti-inflammatory properties of the omega-3 lipid mediator resolvin E3. *The Journal of Biochemistry* **153**: 355-360.
40. Colas, R. A., M. Shinohara, J. Dalli, N. Chiang, and C. N. Serhan. 2014. Identification and signature profiles for pro-resolving and inflammatory lipid mediators in human tissue. *American Journal of Physiology-Cell Physiology* **307**: C39-C54.
41. Zhang, J., Q. Yang, J. Li, Y. Zhong, L. Zhang, Q. Huang, B. Chen, M. Mo, S. Shen, and Q. Zhong. 2018. Distinct differences in serum eicosanoids in healthy, enteritis and colorectal cancer individuals. *Metabolomics* **14**: 1-12.
42. Ferreiro-Vera, C., F. Priego-Capote, and M. L. de Castro. 2012. Comparison of sample preparation approaches for phospholipids profiling in human serum by liquid chromatography–tandem mass spectrometry. *Journal of Chromatography A* **1240**: 21-28.
43. Murphy, R. C., R. M. Barkley, K. Zemski Berry, J. Hankin, K. Harrison, C. Johnson, J. Krank, A. McAnoy, C. Uhlson, and S. Zarini. 2005. Electrospray ionization and tandem mass spectrometry of eicosanoids. *Anal Biochem* **346**: 1-42.
44. Parkinson, J. F. 2006. Lipoxin and synthetic lipoxin analogs: an overview of anti-inflammatory functions and new concepts in immunomodulation. *Inflammation & Allergy-Drug Targets (Formerly Current Drug Targets-Inflammation & Allergy)(Discontinued)* **5**: 91-106.

Acknowledgements

I would like to express my sincerest gratitude to Professor Toshifumi Takao, who always gives me not only a great number of invaluable suggestions and feedback through this work, but also huge unwavering support and heartfelt encouragement throughout my academic journey. I am genuinely grateful for the knowledge and skills I have gained under his mentorship. The whole work was carried out under his supervision in Laboratory of Protein profiling and functional proteomics at Institute for Protein Research, Osaka University.

I would like to express my gratitude to Professor Masayuki Inoue from Laboratory of Synthetic Natural Products Chemistry at Graduate School of Pharmaceutical Sciences, The University of Tokyo for providing the precious Resolvin E3 standards.

I would like to express my gratitude to Professor Michio Murata from Laboratory for Biomolecular Chemistry at Graduate School of Science, Osaka University for the valuable suggestions and fruitful discussions.

I would like to also express my gratitude to Professor Takayoshi Suzuki from Department of Complex Molecular Chemistry at Institute of Scientific and Industrial Research, Osaka University for the valuable suggestions and discussions.

I would like to express my special thanks to Mone Kurokawa and Mengyao Chen, the members of Takao Lab who gave me so many helps on this work.

I am grateful to the financial support from Protein Research Foundation.

I am grateful to Hiroto Akiya and Ko Kanegae, the artists whose stages encouraged me throughout my academic life.

Finally, I am grateful to my parents for their understanding, encouragement and support on this study, especially my mother Caiqin Gu, who is not only a great woman but also a respectable professor from The School of Chemistry and Chemical Engineering, Guangzhou University.